



**COMOTI**  
ROMANIAN RESEARCH &  
DEVELOPMENT INSTITUTE FOR  
GAS TURBINES

# TURBO

Scientific Journal

vol. IV (2017), no. 2

# LASERTEC 30 SLM

## Additive Manufacturing with Selective Laser Melting

- Building Volume (X x Y x Z): 300 x 300 x 300 mm
- Layer Thickness: 20 – 100 µm
- Laser type: Fibre laser
- Integrated powder extraction
- Integrated sieving
- Materials: Titanium Tilop, Inconel 625



## Nikon Altera Bridge CMM 10.10.8



ALTERA's ceramic bridge and spindle components coupled with proven air-bearing design provide the ultimate in stiffness and stability, altogether delivering significantly improved repeatability.

### Features

- Flexible multi-sensor platform: touch probes, analog scanning and laser scanning;
- High capacity (loads) table.

### Benefits

- Premium performance for a 1016 x 1016 x 813 mm area;
- Excellent accuracy 1.8+L/400 micron and repeatability 1.7 micron;
- Total solution for probing, scanning and digital inspection;
- LC60Dx laser scanner ( 9 micron accuracy);
- Powerful Camio and DCC Manager Software with Point Cloud Analysis and Gear measuring and interpretation.

### Applications

- Machined and pressed parts (gears, blades etc);
- Plastic moldings;
- Casting and forgings;
- Touch trigger and non-contact inspection;
- Digitizing, scanning and reverse engineering.

*Cercetarea sau gemenele viitoarelor schimbări*

Se spune că la 11 aprilie 1770 Mozart ajungea în preajma Paștelui, împreună cu tatăl său la Roma. În Capela Sixtină va asculta compoziția corală *Miserere Mei Deus*, bazată pe Psalmul 51, piesă care la câteva zile după ce Gregorio Allegri a compus-o, în jurul anului 1638, a fost protejată prin interzicerea interpretării în afara Capelei Sixtine. Papa impusese cu desăvârșire redarea ei sub amenințarea excomunicării pentru oricine ar fi încercat să copieze lucrarea.

Cu toate acestea micul Mozart transcrie din memorie întreaga piesă corală, după ce o ascultase o singură dată. Va reveni la slujba din Vinerea Mare cu manuscrisul ascuns, pentru a asculta din nou piesa și pentru a face eventuale completări. Papa, surprins de curajul de care a dat dovadă copilul de 12 ani îl cheamă la reședința sa. Teama puștiului a fost repede alungată pentru că Papa i-a zâmbit și i-a spus "Ești un geniu, du-te acasă și scrie muzică!" După această întâmplare Papa a ridicat interdicția copierii și exclusivitatea interpretării în Capela Sixtină.

Oare copilul Mozart a intuit că rezultatul la care un predecesor a ajuns poate fi punctul de plecare pentru ceea ce el însuși avea de clădit?

Lumea de astăzi este o reflectare a cercetării fundamentale de ieri.

Totalitatea materialului acumulat de-a lungul timpului în fiecare ramură a științei a dat naștere cercetătorului, care a procesat mai întâi materialul adunat pentru a crea o imagine a informațiilor la un moment dat, într-un punct de la care să poată porni propria-i muncă de cercetare.

Societatea, adeseori mercantilă, impune cercetarea productivă cu rezultate imediate, utile și rentabile. Cercetarea fundamentală însă, este o cercetare dezinteresată, pe termen lung, fără aplicații practice rapide, ce nu pleacă de la idea de rentabilitate, imprevizibilă din punct de vedere al rezultatelor, însă inițiatoare a progresului și se ascunde adesea în spatele cercetării aplicate. Numai că cercetarea aplicată se bazează pe cercetarea fundamentală, iar cercetarea fundamentală nu poate progresa fără furnizarea progreselor tehnice în cercetarea aplicată.

Progresul tehnic se bazează pe descoperiri fundamentale ale trecutului. Studiul unui fenomen unic, poate genera un lanț de aplicații interdisciplinare, iar astăzi știința are o multitudine de instrumente de accelerare, de îmbunătățire și acumulare de noțiuni fundamentale. Cooperarea este baza progresului în cercetare iar meritul descoperirii unui cercetător este evident al său și al echipei sale. În esență, generațiile anterioare au fundamentat un stoc de informații valide pentru a putea fi susținute noile ipoteze, așa cum noutățile descoperite astăzi vor fundamenta cercetarea generațiilor viitoare.

Cercetarea în sine este deopotrivă purtătoare și generatoare de timp, iar așa cum orice istoric atunci când scrie istorie o alege pe cea care i se potrivește, cum spunea fizicianul și filozoful Gaston Bachelard, orice cercetător va aprofunda domeniul în care se regăsește, sperând, de ce nu, la acel adevărat gemenă fericit al viitoarelor schimbări.

*„Noroc este atunci când cauți un ac într-un car cu fân și descoperi fiuca fermierului!”*

*Julius H. Comroe*

*Autor: Elena Banea*

*Research or the Seed of Future Changes*

It is said that on April 11th 1770, Mozart and his father reached Rome during the Easter time. Inside the Sistine Chapel he listened to the choir composition Miserere Mei Deus, inspired by the 51st Psalm, a musical work that was to be protected only a few days after Gregorio Allegri composed it (around year 1638) by the interdiction to be played outside the Chapel. The Pope had absolutely banned its reproduction under the threat of excommunication of anyone who would have tried to copy it.

Nevertheless, young Mozart transcribes the complete choir piece by heart after only one audition of it. He returned to the Holy Friday service with the hidden manuscript on him in order to listen to it once again and possibly bring some changes to it. Surprised by the twelve-year-old child's courage, the Pope summoned him to his residence. The boy's fear was to be soon banished when the Pope smiled to him and said: „You are a child prodigy, go home and write music!“ After that event, the Pope removed the ban of its transcription and of the exclusive interpretation of the piece inside the Sistine Chapel.

Could young Mozart possibly guess that the result a predecessor had reached before might be a starting point for what he himself was to create?

Today's world is a reflection of yesterday's fundamental research.

The whole amount of work accumulated in time in each branch of science has made the research worker, who first processed the existent material in order to get a bird's eye-view of the information existent at a specific moment, and reach a point from which he could start his own research work.

Society, mercantile as it often is, asks for productive research with immediate, useful and profitable results. Though fundamental research is done for its own sake, in the long run and without immediate practical use, it does not include the idea of profitableness, it is unpredictable as far as the results are concerned, yet it promotes progress and it often backs applied science. The problem is that applied research depends on fundamental research, while the latter cannot register any progress without offering new technical solutions to applied research.

Technical progress is based on fundamental discoveries of the past. The study of a unique phenomenon can generate a whole range of interdisciplinary practical ends, the more so as science is capable of generating today a multitude of instruments to accelerate, improve and archive fundamental knowledge. Cooperation is the basis of progress in research work, and the merit for a particular discovery definitely belongs to a specific research worker and to his/her team. Basically, previous generations have laid the basis for a stock of valid information in order to sustain the new hypotheses, similarly as today's discoveries will fundament the next generations' research.

Research, in itself, is both time carrying and time generating. In the same way as any historian who writes history chooses one which best suits him, as the physician and philosopher Gaston Bachelard used to say, any research worker is sure to study thoroughly his own field of activity, hopefully searching for the true seed of future changes.

*„Serendipity is looking in a haystack for a needle and discovering a farmer's daughter! “*

*Julius H. Comroe*

*Author: Elena Banea*

## EDITORIAL BOARD



### **PRESIDENT:**

Dr. Eng. Valentin SILIVESTRU

### **VICE-PRESIDENT:**

Dr. Eng. Cristian CĂRLĂNESCU

Dr. Eng. Romulus PETCU

### **SECRETARY:**

Dr. Eng. Jeni POPESCU

### **MEMBERS:**

Prof. Dr. Virgil STANCIU

Prof. Dr. Corneliu BERBENTE

Prof. Dr. Dan ROBESCU

Prof. Dr. Sterian DĂNĂILĂ

Dr. Eng. Gheorghe MATACHE

Dr. Eng. Ene BARBU

Eng. Gheorghe FETEA

Dr. Eng. Ionuț PORUMBEL

Dr. Eng. Mircea Dan IONESCU

Dr. Eng. Lucia Raluca VOICU

Dr. Eng. Mihaella CREȚU

Dr. Eng. Cleopatra CUCIUMIȚA

Eng. Sorin GABROVEANU

### **EDITOR IN CHIEF:**

Prof. Dr. Lăcrămioara ROBESCU

### **EDITORS:**

Eng. Mihaela Raluca CONDRUZ

Iulia VOINEA

Ec. Elena BANEA

### **ADMINISTRATIVE SECRETARY:**

Eng. Mihaela GRIGORESCU

### **TRANSLATION CHECKING:**

Dr. Eng. Paul RĂDULESCU

Laura COMĂNESCU

Oana HRIȚCU

### **GRAPHICS:**

Victor BEȘLEAGĂ

More information regarding the scientific journal can be found at:

[http://www.comoti.ro/ro/jurnalul\\_stiintific\\_turbo.html](http://www.comoti.ro/ro/jurnalul_stiintific_turbo.html)

[turbojournal@comoti.ro](mailto:turbojournal@comoti.ro)

[jeni.popescu@comoti.ro](mailto:jeni.popescu@comoti.ro)

**ISSN: 2559-608X**

**ISSN-L: 1454-2897**

The articles from this journal cannot be copied or republished without the editorial's board permission.

## TABLE CONTENT

### AUTOMATION AND MONITORING

Behaviour of a wireless connection during traffic conditions within an industrial environment

Mitru A., Borzea C..... pp. 4

Diagnosing of rotary blade machines with the HolderPPS system

Niculescu F., Vilcu C., Borzea C..... pp. 8

### MATERIALS AND TECHNOLOGIES

Self-healing efficiency for fiber reinforced polymer composites

Vintilă, S., Condruz R., Paraschiv A..... pp. 14

Evaluation of mechanical properties of carbon nanotube reinforced composites

Condruz M.R., Vintilă S., Paraschiv A ..... pp. 19

### COMPRESSORS, BLOWERS

Numerical investigation of a screw compressor performance

Mălăel I., Sima M. .... pp. 25

### RENEWABLE ENERGY AND RECOVERY

Screw expander tested on comoti bench and at beneficiary

Petrescu V., Toma N., Slujitoru C. .... pp. 31

### TRIBOLOGY, DIAGNOSIS, ACOUSTICS AND VIBRATIONS

Fault diagnosis of aircraft gas turbine engine by vibration analysis

Flore L. .... pp. 37

# BEHAVIOUR OF A WIRELESS CONNECTION DURING TRAFFIC CONDITIONS WITHIN AN INDUSTRIAL ENVIRONMENT

Andrei MITRU<sup>1</sup>, Claudia BORZEA<sup>1</sup>

**ABSTRACT:** The paper describes a Wi-Fi equipment hardware configuration intended for testing of a remote communication system with a terminal, which is part of an automation system belonging to a test bench. The experimentation of the Wi-Fi connection is carried out with the test bench working. The communication path crosses the working test bench and many other devices in operating state. In this way, industrial environment conditions are fulfilled. One of the purposes of the paper is to evaluate the parameters considered for the implementation of a system based on Wi-Fi technology, for data remote transmission from the test bench terminal. Setting the parameters for a system based on Wi-Fi technology is useful for the analysis of the behaviour of a Wi-Fi connection within an industrial environment and represents an expected result by providing the continuity and integrity of the transmitted data. The presentation of signal behaviour test results of a type of connection between Wi-Fi devices, in an industrial environment, represents another objective of the paper. Developing a method of evaluation for the behaviour of the Wi-Fi connection in industrial environment through the analysis of the parameters resulted from computation or tests represents an expected outcome. The testing configurations and techniques using specialized software applications are also presented.

**KEYWORDS:** Wi-Fi Technology, Communication System, Remote Transmission, Industrial Environment, Data Traffic, Test Bench.

## NOMENCLATURE

CCQ - Client Connection Quality  
FM - Frequency Modulation  
FSPL - Free Space Path Loss  
 $G_R$  – Received signal antenna gain  
 $G_T$  – Transmitted signal antenna gain  
RSL - Received Signal Level  
RSLM - Minimum level of the received signal  
RSSI - Received Signal Strength Indicator  
 $R_X$  Packet – Packets Received on the terminal  
SNR - Signal to Noise Ratio  
TSL - Transmitted Signal Level  
 $T_X$  Packet - Packets Transmitted out the terminal  
WLAN - Wireless Local Area Network  
d - Distance between the devices  
f - Signal frequency

## 1. INTRODUCTION

Developing an efficient method by making an analysis of the parameters from a signal and trace that signal with a software solution in real time is important in the following activities which are performed

---

<sup>1</sup> National Research and Development Institute for Gas Turbines COMOTI, Bucharest, Romania

by having the described Wi-Fi network as a support:

- development of a remote communication diagram for test benches and for automation equipment used by beneficiaries;
- designing of hardware structures for the automation systems that are part of test benches and of equipment which is subject for the automation part used by beneficiary;
- analysis of hardware and software structures for data transmission;
- development of control algorithms, protection and shutdown algorithms, start and stop algorithms for bladed machines;
- realization, visualization and analysis of remotely transmitted displays to trained personnel in charge with the monitoring of the installation;
- obtaining a series of results for the conducted tests with the instruments that the remote communication systems will be equipped with;
- observing the behaviour of the remote data transmission system in various situations when unpredicted events interfere upon a test bench;
- establishing security solutions for remote data transmission.

## 2. HARDWARE ARCHITECTURE AND PARAMETER CALCULATION

The set of experiments consider a started test bench and a connection with two identical Mikrotik GROOVE A-52HPn [1] devices (Fig. 1). For the communication channel there will only be considered the support from a line based on a WLAN network, according to the standard IEEE 802.11. [2]

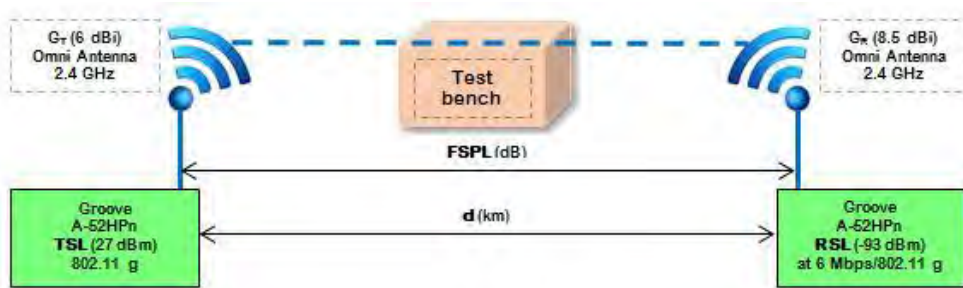


Fig. 1 The Wi-Fi connection for experimental purpose

It will be considered that the distance between the devices is  $d = 0.05$  km and the signal frequency is  $f = 2.4$  GHz. The free space path loss parameter is hereinafter calculated: [3]

$$FSPL[dB] = 20 \log_{10} d [km] + 20 \log_{10} f [GHz] + 92.45 \quad (1)$$

$$FSPL[dB] = 73.98 dB \quad (2)$$

Within this type of connection proposed, the values of the transmitter parameters are: transmitted signal level  $TSL [dBm] = 27$  dBm and antenna gain  $G_T [dBi] = 6$  dBi. The receiver parameters in the technical specification are: receiver antenna signal amplification with the antenna gain factor  $G_R [dBi] = 8.5$  dBi, and the received signal level  $RSL = -93$  dBm.

The reception signal level RSL will be calculated to see if its value fits within the limits so that the signal can be received, taking into account the free space path loss which was previously inferred: [3]

$$RSL[dBm] = TSL[dBm] + G_T[dBi] - FSPL[dB] + G_R[dBi] \quad (3)$$

$$RSL[dBm] = -32.48 dBm \quad (4)$$

In case of fluctuations and considering that the frequency modulation is  $FM = 12$  dB-Hz, the minimum level of the received signal is:

$$RSLM[dBm] = RSL[dBm] - FM[dBHz] \quad (5)$$

$$RSLM[dBm] = -44.48 \text{ dBm} \quad (6)$$

Using a low power transmitter with a high gain antenna is much more convenient than vice versa, because from the connection cost formula it can be observed that the transmitted power level can be achieved in various ways, but the WLAN device is, in the same time, both transmitter and receiver. In this situation, regardless of the signal transmission power, the only factors that matter are the antenna gain and the receiver sensitivity.

### 3. SOFTWARE SOLUTION AND EXPERIMENTATION SETUP

For the test configuration, a terminal provided with Winbox application will be connected to the communication device that receives the Wi-Fi signal. At the other end, another terminal is connected to the Wi-Fi equipment. A simulated traffic is performed between the two terminals using the Wi-Fi communication route. By means of certain instruments within Winbox application, a radio analysis of the signal will be performed.

The tests are conducted with a test bench in operation mode. The bench is situated within the communication channel. While conducting these tests, along the communication channel there are also devices such as converters and transformers which are electrically supplied. Considering these facts, the test conditions in industrial environment are fulfilled.

The test bench is firstly started up, which supposes the start-up of the main direct current motor driving the bench installation and of certain other motors driving oil pumps. The setup of the communication route was purposely made so that the radio waves transmission to be performed with the entire test bench in its way.

Once the terminal is connected to the communication device, "Interfaces" section is accessed in Winbox application, where "WLAN" connection is selected. In this way, all the properties for this connection will be accessed and the features can be visualized and compared.

### 4. RESULTS

After the continuous transmission of 137 data units, there were no signal losses found during transmission, and neither on reception. The transmission is done at a data package rate varying around 40 packages per second. The rate of received packages also varies and is around the value of 35 packages per second. The speed rate of the data transmission is around 415 Kb/s.

When the data transmission has reached 195 data units, small losses of the signal level are being noticed. These losses are rare though and do not imply data loss. The transmission and the reception are done at a data package rate varying around 35 packages per second.

During message transmission, the characteristic signal parameters are also displayed. The following parameters can be thus identified: MAC address of the communication device, received signal strength indicator RSSI = -44 dBm, client connection quality CCQ = 89% and signal to noise ratio SNR = 63 dB.

When reaching 406 data units, the signal graph indicates no loss and a relative uniformity of the data packages transmission, which varies around 34 packages per second.

When the data transmission is reaching the level of 601 data units (Fig. 2), short signal losses are identified in the signal graph. Like the previous ones, these signal losses do not lead to data loss. The transmission is done at a rate varying around 35 packages per second.

Comparing to the characteristic signal parameters identified to 251 data units, it can be noticed that the RSSI level increases from -44 dBm to -43 dBm, the CCQ indicator decreases from 89% to 84%, and the signal to noise ratio rises from 63 dB to 64 dB.



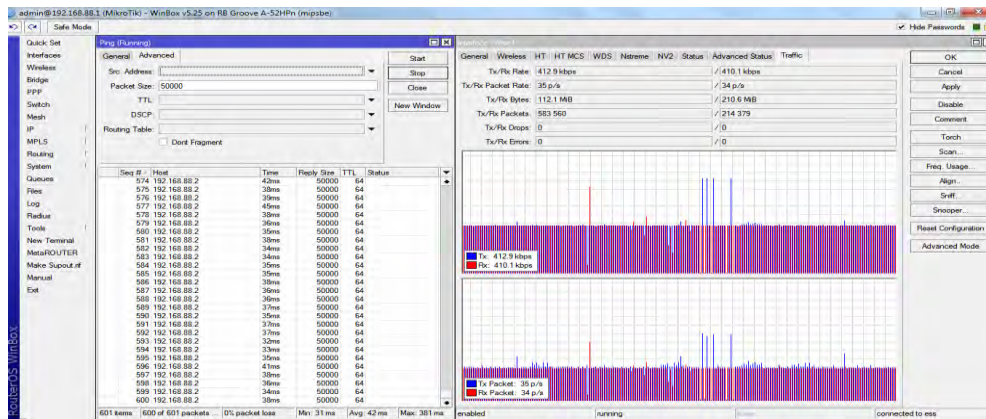


Fig. 2 Signal analysis at 601 data units sent

## 5. CONCLUSIONS

The novelty of the paper consists in the methods selected for performing an analysis of the signal behaviour during data transmission within an industrial environment. These methods are applied from the beginning, by choosing communication equipment in such a manner so that implementing the hardware configuration and making the necessary parameter calculations will make possible to notice any signal change during experimentation.

The small distance of 50 meters between the Wi-Fi equipment and using two devices having an omni external antenna with a higher reception gain decisively contributed to the positive results in insignificant signal losses and to no data package loss for the tested connection, with the operating test bench within the industrial environment.

The antenna gain is important during both transmission and reception of the signal for its quality. The experimental communication system aims only on carrying out a correct data transmission considering the fact that the environment is affected by electromagnetic influences specific to industrial environment.

After achieving these positive results, the experimental connection tested was afterwards left to operate for the remote communication through radio waves with the test bench, having the possibility to be further extended.

## ACKNOWLEDGEMENT

This work was carried out within “Nucleu” Program TURBO 2020, supported by the Romanian Minister of Research and Innovation, project number PN 16.26.07.02.

## REFERENCES

- [1] “Mikrotik Groove 52”, Mikrotik.Com, 2017, <https://mikrotik.com/product/RBGroove52HPnr2>;
- [2] Bradley Mitchell, ”Wireless Standards 802.11A, 802.11B/G/N, And 802.11Ac”, Lifewire, 2017, <https://www.lifewire.com/wireless-standards-802-11a-802-11b-g-n-and-802-11ac-816553>;
- [3] Sorin Puşoci, Sorin Soviany, Viorel Manea, Andrei Scheianu, “Sistem de măsurare a stabilității transmiției datelor, cu conexiune wi-fi, în mediu industrial” (“Measuring System for Data Transmission Stability, with Wi-Fi Connection, within Industrial Environment”), 2015

## DIAGNOSING OF ROTARY BLADE MACHINES WITH THE HolderPPS SYSTEM

Filip NICULESCU<sup>2</sup>, Constantin VÎLCU<sup>2</sup>, Claudia BORZEA<sup>2</sup>

**ABSTRACT:** HolderPPS system was designed with the purpose of monitoring continuously, dynamically, the mechanical system of rotary blade machines. Conceived as an operational element in the proactive maintenance of RBM, the HolderPPS system enables to perform a continuous and dynamic surveillance of the operational status of all the elements of the mechanical system. Therefore, in the given conditions of the industrial process where the machine is used, the inchoate operation faults can be managed beforehand. The monitoring results of each bladed machine investigated will be stored in a data base, which tends towards building a knowledge base. A history will be thus created by accumulating an information volume, with great usefulness for a periodic analysis of the main causes of RBM faults. Measures can be taken in this moment for avoiding future faults or failures. Such an approach is called proactive, and will be conducted on medium and long term, leading to costs savings regarding machine exploitation.

**KEYWORDS:** HolderPPS, Rotary blade machine, Proactive maintenance, Machine performance, Operation monitoring, Fault avoiding, Costs savings

### NOMENCLATURE

CU 90 – Screw compressor type produced by COMOTI

HolderPPS – Data recorder system for proactive maintenance to rotary blade machines;

ID – Identity Document;

IR – Infrared;

RBM – Rotary Blade Machine;

RC – Current revision;

RK – Capital revision;

RT – Technical revision;

RTD – Resistance Temperature Detector.

### 1. INTRODUCTION

The modern characterization of a product is realized relying on: the level of technical performances, reliability, maintainability and availability indicators, maintenance support, costs for product possession and other requirements for a safe operation. Thus it is possible to define an overall efficiency of the product. An effective maintenance strategy has the role of reducing downtimes, of detecting accurately and beforehand the possible causes that can lead to malfunctions, of simplifying as much as possible the actions carried out for the remediation of these issues, and of reducing their impact on the industrial process. The maintenance strategies are as follows: corrective, programmed, preventive, predictive and proactive.

The reliable manufacturers of rotary blade machines recommend, from the point of view of optimum ratio [reliability/overall maintenance cost], a proactive maintenance approach. This is to be performed from the moment of running in the machine continuously on the entire functional exploitation period, for obtaining an excellent reliability with reduced costs. This approach is found in the speciality literature and is illustrated in Figure 1 showing maintenance costs in the first years of operation of mechanical plants including rotary blade.

---

<sup>2</sup> National Research and Development Institute for Gas Turbines COMOTI, Bucharest, Romania

machines. Solid solutions require time, anticipation, patience and discipline. Current investments for the management of maintenance strategies are directed towards an overall maintenance by the proactive maintenance.

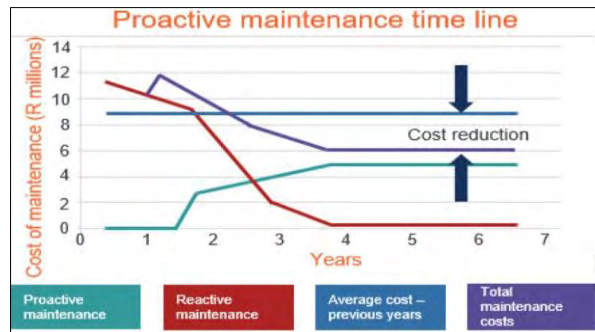


Fig. 1 – Diagram of maintenance costs in the first years of operation of mechanical plants [1]

## 2. PAPER CONTENTS

Predictive maintenance is a technique that allows for a systematic method of monitoring and trending of equipment condition. This activity takes place while equipment is on-line and provides early warning of equipment operation approaching out of limit conditions. [2]

While predictive maintenance uses online condition monitoring to help predict when a failure will occur, it doesn't always identify the root cause of the failure. That's where proactive maintenance comes in. Proactive maintenance relies on information provided by predictive methods to identify problems and isolate the source of the failure. [3]

The proactive maintenance ensures the transition towards an overall maintenance of RBM. The realization of a product or a rotary blade machine is characterized by an effectiveness coefficient within the industrial technological process where this one is operating and for which it was designed. This coefficient is defined globally as product effectiveness and represents a modern characterization of RBM, as a function of multiple variables: level of technical performances, indicators of reliability, maintainability and availability, maintenance support, costs for product possession, other requirements for a safe operation, etc.

To obtain a maximum effectiveness for the RBM product, an integrated management of the proactive maintenance is practiced since the product conception stage, according to the diagram in Figure 2. Thus, COMOTI achieved the performance of designing and manufacturing electric driven screw compressors for natural gas compression, which recorded a continuous functioning without RK of over 80,000 hours.

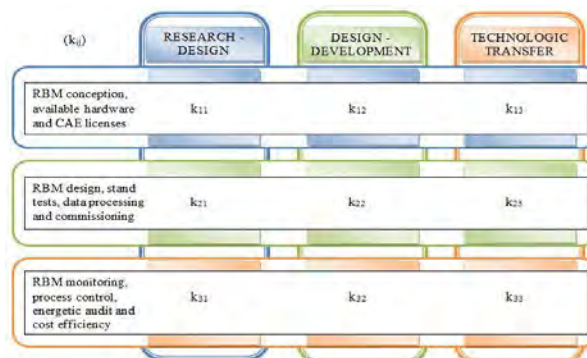


Fig. 2 – Logistic flux diagram for proactive maintenance of COMOTI RBM

## 3. MATHEMATICAL MODEL

The matrix assigned to the diagram in Figure 2 is:

$$M_p = \begin{bmatrix} k_{11} & k_{12} & k_{13} \\ k_{21} & k_{22} & k_{23} \\ k_{31} & k_{32} & k_{33} \end{bmatrix} \quad (1)$$

The coefficients ( $k_{ij}$ ) take values in the interval  $(0 \div 1)$  on a scale defined qualitatively as follows:

$$\begin{aligned} (k_{ij}) = 1.00 & \quad \text{for excellent rating;} \\ (k_{ij}) = 0.80 & \quad \text{for very good rating;} \\ (k_{ij}) = 0.60 & \quad \text{for good rating;} \\ (k_{ij}) = 0.40 & \quad \text{for moderate rating;} \\ (k_{ij}) = 0.20 & \quad \text{for unsatisfactory rating;} \\ (k_{ij}) = 0.00 & \quad \text{for poor rating;} \end{aligned} \quad (2)$$

Depending on the evaluation of every corresponding indicator in Figure 2, the values (2) for  $k_{ij}$  coefficients are estimated and introduced in (1) for a COMOTI rotary blade machine (screw compressor, blower, centrifugal compressor, etc.). The evaluation is performed in real research and development conditions for its realization as prototype or functional model. The absolute value of the determinant assigned to  $M_p$  matrix of integrated management has a below unit value for a deficient management, and respectively an over unit value for a good management. Hereinafter, the integrated management of proactive maintenance is evaluated qualitatively for a specific case of RBM, namely a screw compressor.

$$\|M_p\| = \begin{vmatrix} 0.6 & 0.8 & 0.4 \\ 0.8 & 0.4 & 0.2 \\ 0.6 & 0.8 & 1.0 \end{vmatrix} = \|0.592 - 0.832\| = \|-0.24\| = 0.24 > 0.2 \quad (3)$$

In the case of the engine driven screw compressor type MCS 15.6 model COMOTI, the value of the determinant was calculated after replacing the  $k_{ij}$  with the real values for product realization. The result given in equation (3) was obtained, for which the rating is *unsatisfactory*. This result has determined approaching the thematic in connection with the elaboration of a mathematical model as a logistic base regarding the management of proactive maintenance for RBM. Within NUCLEU program, the logistic flux was elaborated for the automation designing of RBM type machines, with the integration of predictive/proactive maintenance even since the commissioning stage. In this regard, the IR thermal print and the characteristic vibrations of the machine which occur during operation become “reference zero” in the knowledge base for each RBM.

For the RBM type machines realized by INCD Gas Turbines COMOTI and commissioned to the beneficiary, an electronic maintenance sheet is elaborated with the corresponding ID of the RBM. The sheet allows the real time recording of the machine operation data, both for programmed maintenance (RC, RT, RK), as well as for predictive maintenance. The sampling data is introduced in the knowledge base of the RBM and enables a highly realistic and trustworthy evaluation regarding the diagnose of RBM condition at a given time, and an estimation of the remaining operation time.

#### 4. WORKING METHODOLOGY

Hereinafter, the methodology for diagnosing of the RBM – engine driven screw compressor type MCS 15.6 – designed, realized and commissioned as demonstrative model at the natural gas compression plant Rafles Energy SRL in the location Frătăuții Noi – Rădăuți. The working methodology regarding diagnosing a rotary blade machine with HolderPPS system consists of the following steps, as follows:

##### A. Identification of rotary blade machine

- Rotary blade machine: *Compressor MCS-15.6*;
- Operating location in the process: *Frătăuții Noi – Rădăuți*;
- Operating hours: *16525*;
- Diagnosing date: *07.09.2017*.

**Table 1. Technical features**

I – RBM driving engine Technical features			II –RBM compressor Technical features			III – RBM skid systems Technical features		
1.1	Engine type	Thermal Caterpillar	2.1	Compressor type	Screw	3.1	Outlet separator vessel [PN]	600 [l]
1.2	P.N. engine	G3304-NA	2.2	P.N. compressor	CU 90	3.2	Oiling system [PN]	Under pressure
1.3	Driving shaft power [kW; HP]	71 [kW]	2.3	Max. power consumed [kW; HP]	70 [kW]	3.3	Oil cooling system [PN]	With radiator
1.4	Engine shaft coupling	Flexible	2.4	Skid mounting	Rigid	3.4	FSA – Inlet separator filter [PN]	400 [l]
1.5	Skid mounting	Elastic (dampers)	2.5	---	---	3.5	FSR – Outlet separator filter [PN]	600 [l]
1.6	---	---	2.6	---	---	3.6	RBM skid bed frame	welded
1.7	Fabrication year	1990	2.7	Fabrication year	2010	3.7	Fabrication year	2008

**A. RBM functional and process parameters**

**Table 2. RBM parameters**

T <sub>lr</sub> [°C]	P <sub>gc</sub> [bar]	I / U [A/V]	P <sub>ui</sub> [bar]	T <sub>ui</sub> [°C]	T <sub>us</sub> [°C]	T <sub>grc</sub> [°C]	v <sub>r</sub> mm/s	P <sub>ga</sub> [bar]	T <sub>ga</sub> [°C]	P <sub>gr</sub> [bar]	T <sub>gr</sub> [°C]	Q <sub>gr</sub> [Nm <sup>3</sup> S]
87	0.234	7,89 / 400	3.57	47.5	35.8	67.8	---	0.65	25.7	8.57	34.5	456.00

\*where: T<sub>lr</sub> – outlet bearing temperature; P<sub>gc</sub> – compressor gas pressure; I/U – electric current/voltage; T<sub>ui</sub> – oil inlet temperature; T<sub>us</sub> – separator oil temperature; T<sub>grc</sub> – compressor outlet gas temperature; v<sub>r</sub> – radial vibrations; P<sub>ga</sub> – inlet gas pressure; T<sub>ga</sub> – inlet gas temperature; P<sub>gr</sub> – outlet gas pressure; T<sub>gr</sub> – outlet gas temperature; Q<sub>gr</sub> – outlet gas flow.

**B. RBM vital parameters**

**Table 3. Vital parameters monitored for RBM condition – proactive maintenance**



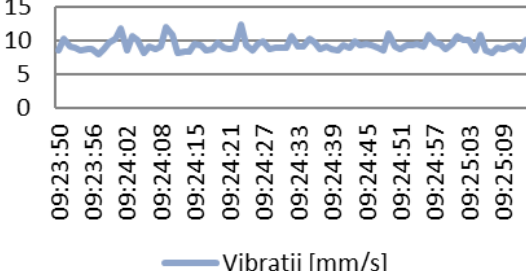

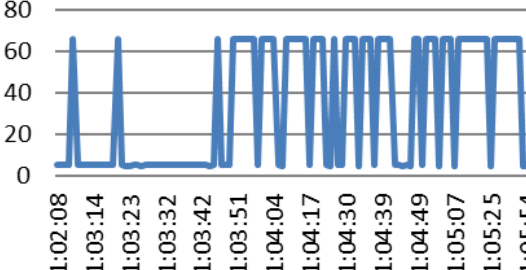

RBM driving engine			RBM compressor			RBM skid systems		
v <sub>m1</sub>	Engine head vibrations	27.00 mm/s	v <sub>c1</sub>	Driving bearing vibrations	9.75 mm/s	v <sub>s1</sub>	FSA inlet filter vibrations	2.34 mm/s
v <sub>m2</sub>	Engine casing vibrations	27.00 mm/s	v <sub>c2</sub>	Compressor casing vibrations	11.75 mm/s	v <sub>s2</sub>	FSR outlet filter vibrations	3.45 mm/s
v <sub>m3</sub>	Driving bearing vibrations	17.00 mm/s	v <sub>c3</sub>	Outlet head vibrations	12.50 mm/s	v <sub>s3</sub>	RBM skid vibrations	3.00 mm/s
T <sub>m1</sub>	Engine head temp.	85.00 °C	T <sub>c1</sub>	Driving bearing vibrations	44.00 mm/s	T <sub>s1</sub>	FSA gas temp.	21.00 °C
T <sub>m2</sub>	Engine casing temp.	60.00 °C	T <sub>c2</sub>	Compressor casing temp.	39.00 °C	T <sub>s2</sub>	FSR gas temp.	39.00 °C
T <sub>m3</sub>	Driving bearing temp.	40.00 °C	T <sub>c3</sub>	Gas outlet head temp.	57.00 °C	T <sub>s3</sub>	Skid bed frame temp.	19.00 °C
C <sub>um</sub>	Lube oil quality	90 %	C <sub>uc</sub>	Lube oil quality	70 %	C <sub>uvs</sub>	Lube oil quality	70 %

A comprehensive predictive maintenance program is composed of several techniques which, when combined, can predict most mechanical and electrical problems found in equipment [2]. Several investigation methods have been employed for vibration, temperature and lubrication oil quality analysis, combined with visual on-site inspection. For oil quality evaluation, samples are taken and off-line laboratory analyses are carried out to establish its level of degradation.

**C. RBM vibration analysis**

Vibration analysis [...] is performed on mechanical equipment to evaluate the on-line condition of its mechanical parts, and effect on related pieces of equipment. Effectiveness of vibration mounts, shafts, bearings, coupling alignment and impeller balance are measured and monitored to determine if equipment is functioning properly and within specifications. [2]

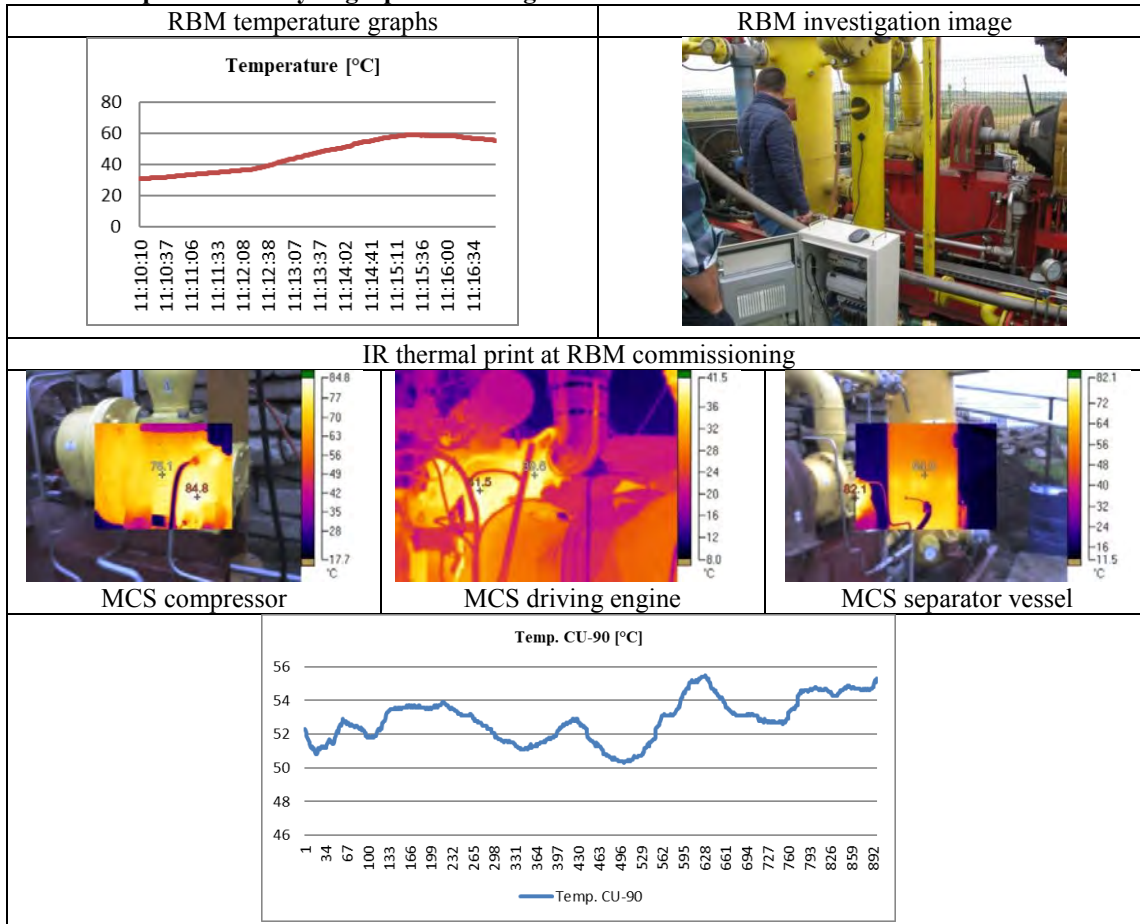
**Table 4. Vibration analysis graphs and images**

RBM vibration graphs	RBM investigation image
	
<p><b>CU 90 - Vibrations [mm/s]</b></p>  <p>— Vibratii [mm/s]</p>	
<p><b>RTD vibrations [mm/s]</b></p> 	

**D. RBM temperature analysis**

Thermography is used to analyse equipment that exhibits over-heating and heat links when not operating properly. [2]

**Table 5. Temperature analysis graphs and images**



## 5. CONCLUSIONS

The paper presents the elaboration of a logistic base with its stages and activities considered for the management of proactive maintenance for rotary blade machines. HolderPPS system monitors continuously, dynamically, the operating parameters of the equipment (pressures, temperatures, flows, vibrations, level, valves position, electric current, etc.). Thus, it enables to detect beforehand the potential problems that can lead to a faulty operation or that can reduce the lifetime of the machine. HolderPPS system ensures the identification of the faults, as well as of the optimum measures for the adequate remediation of these faults.

## ACKNOWLEDGEMENT

This work was carried out within “Nucleu” Program TURBO 2020, supported by the Romanian Minister of Research and Innovation, project number PN 16.26.03.01.

## REFERENCES

- [1] "Mechanical Applications - MARTEC", *MARTEC*, last modified 2017, <http://www.martec.co.za/mechanical/>;
- [2] NASA, *Predictive Maintenance-Facility, Ground Support Equipment*, eBook, n.d., <https://oce.jpl.nasa.gov/practices/ops13.pdf>;
- [3] Emerson, *Maintenance 101: Understanding Maintenance Strategies*, eBook, 2002, <http://www2.emersonprocess.com/siteadmincenter/PM%20Central%20Web%20Documents/Bus%20Sch-MAINT101.pdf>;

## SELF-HEALING EFFICIENCY FOR FIBER REINFORCED POLYMER COMPOSITES

Sebastian VINTILA<sup>3</sup>, Raluca CONDRUZ<sup>3</sup>, Alexandru PARASCHIV<sup>3</sup>

**ABSTRACT:** The paper presents a study on self-healing behaviour of fibre reinforced composite materials integrating dicyclopentadiene filled urea-formaldehyde microcapsules as healing system and Grubb's catalyst as reaction catalyst. Microstructural analysis showed the formation of microcapsules with diameter ranging from 100  $\mu\text{m}$  to 200  $\mu\text{m}$ . Composite samples were manufactured using prepreg plies and 5%wt. Grubb's catalyst and 10%wt. microcapsules and subjected to three point bending flexural test (according to SR EN ISO 14125). Samples showed a healing recovery of 87-94% after second loading, after they were left at 35°-40°C for the healing to take effect

**KEYWORDS:** composite materials, self-healing, thermoset polymers, microcapsule

### NOMENCLATURE

DCPD – Dicyclopentadiene  
EMA – Ethylene Maleic Anhydride  
HCl – Hydrochloric Acid  
NaOH – Sodium Hydroxide  
NH<sub>4</sub>Cl – Amonium Chloride  
NRDI – National Research and Development Institute  
OM – Optical Microscopy  
RPM – Rotations per Minute  
RT – Room Temperature  
SEM – Scanning Electron Microscopy  
UF – Urea-Formaldehyde  
f – Property of interest  
 $\eta$  – Healing Efficiency

### 1. INTRODUCTION

Self-healing materials draw inspiration from biological processes in nature, have been generating much research interest, and are promising candidates for a new generation of engineering materials with extended service life, reduced cost associated with repair and maintenance, and improved durability and reliability. The resilience of these materials enables them to be employed with a greater confidence factor, even in critical applications such as in the structural elements of aircraft [1,2] Self-healing composite material is a newly emerging damage management concept of this decade, where the damage in the material disappears spontaneously. The empty space of the crack or defect needs to be filled with a new matter called 'healing agent', which not only moves to the damage site, but also bonds the damage surface permanently. For the healing agents to remain in its state until the damage occurs and get changed to a different state to bond the surfaces after damage, a trigger is needed to initiate the self-healing process [3,4].

In a study conducted by Neisiany [5], core-shell nanofibers encapsulating healing agents were fabricated via the facile and economical coaxial electrospinning method and were incorporated in carbon

---

<sup>3</sup> National Research&Development Institute for Gas Turbines COMOTI



fiber/epoxy composite panels to imbue them with self-healing ability. The encapsulation of healing materials in core-shell nanofibers has gained attention in 2010 based on its ability to overcome the adverse side effects of encapsulation in capsule-based and microchannel based systems, strategies which have been investigated since 2001. Two types of poly-methyl-methacrylate (PMMA) shell based nanofibers were fabricated, one with an epoxy resin core, the other with an amine-based curing agent core. Mechanical tests showed that embedding the PMMA core-shell nanofibers between carbon fiber layers led to an increase both in the in-plane and out-of-plane properties of the hybrid composites, but did not have significant effect on impact absorption energy. The results indicated the incorporation of core-shell nanofibers containing healing agents not only improved the initial mechanical properties, but also resulted in self-healing carbon fiber-epoxy composites which were able to recover its initial mechanical properties up to four times after sustaining damage to failure. Ahangaran [6] has prepared poly-methyl methacrylate (PMMA) microcapsules filled with epoxy prepolymer, 3-aminomethyl-3,5,5-trimethylcyclohexylamine and pentaerythritol tetrakis (3-mercaptopropionate) as healing agents for self-healing purposes. PMMA with two different molecular weights ( $M_1 = 36,000$  g/mol and  $M_2 = 550,000$  g/mol) were used with two types of different emulsifiers (ionic and polymeric) to prepare microcapsules. The authors have found that PMMA microcapsules separately filled with epoxy and amine had core-shell morphologies with smooth surfaces. The mercaptan/PMMA particles exhibited core-shell and a corn-shape morphology. The surface morphology of mercaptan microcapsules changed from holed to plain in different emulsion systems. The theoretical equilibrium morphology of PMMA microcapsules was predicted according to spreading coefficient values of phases in emulsion systems. Ahangaran [6] concluded that the surface morphology of PMMA microcapsules depended strongly on the nature of the core, molecular weight of PMMA, type and concentration of emulsifier.

In another study done by Neisiany [7], a self-healing carbon/epoxy composite was fabricated with the incorporation of healing agent loaded core-shell nanofibers between carbon fiber fabric layers. The healing agents, consisting of two components, a low viscosity epoxy resin and its amine-based curing agent, were encapsulated in Styrene acrylonitrile (SAN) nanofibers via a coaxial electrospinning method. The average nanofiber diameters were 750 and 670 nm for the epoxy and amine-based curing agent cores, respectively. The authors mentioned that mechanical studies (three-point bending tests) of the hybrid composite showed that embedding the fabricated core-shell nanofibers did not lead to a reduction in the mechanical properties of host composite, which was corroborated with statistical analysis. A 24 h time interval between each cycle of breakage and healing was considered, allowing sufficient time for the reaction between the healing agents and matrix to go to completion, before the second load for three-point bending test. Neisiany [7] has reported that the healing efficiency of flexural strength indicated a composite recovery between 89% and 97%. Mechanical evaluations and curing behavior studies both showed that incorporation of the aforementioned nanofibers between carbon layers can imbue the conventional carbon/epoxy composite with a self-healing ability, allowing it to repair itself to restore its mechanical properties for up to three cycles at room temperature in absent of any external driving force. Luterbacher et al. [8] has successfully implemented vascular self-healing technology into a simplified strap lap specimen, showing that the introduction of a vascular microchannel reduces the strength by 15%, but having little effect on the stiffness. Upon delivery and cure of epoxy-based self-healing agents full recovery of the mechanical properties was observed. Luterbacher has further implemented this self-healing approach, to larger stringer run-out panels as a feasibility study, in which no knockdown to mechanical properties were caused by the embedded vascular microchannels.

Saini has reported [9] experimental investigations on the self-healing mechanism inside carbon fibre reinforced polymer composites. For the self-healing purpose the specimens were prepared with ingenious hollow glass capillaries to serve the healing agent locally at the sight of failure. The specimens were subjected to cyclic flexural loading first to get a pre-healed specimen and then loaded in the subsequent cycles post healing. The strength of healed specimen was finally compared with the strength virgin specimens having no self-healing mechanisms for the reference purpose. The authors have reported that the healing efficiency was observed between 45%-55% for different set of healing times.

## 2. EXPERIMENTAL SETUP

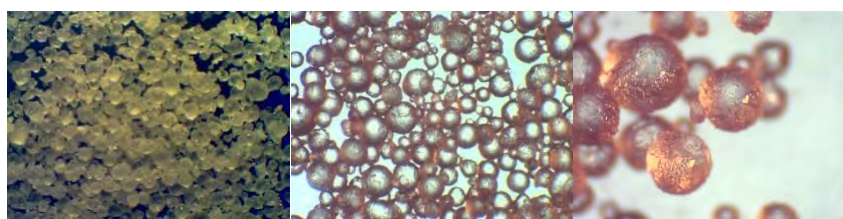
For the fabrication of healing system, an in-situ polymerization method was used, following White's [10] methodology. This fabrication methodology was appointed by many authors and cited in many scientific papers. Materials used for microcapsule fabrication are presented in Table 1. Dicyclopentadiene, Urea, Formaldehyde, Ethylene Maleic Anhydride copolymer and all other chemicals were purchased from Sigma-Aldrich. DCPD was purchased in its monomer form which is a crystalline solid at room temperature and which

melts at 32.5°C. Also, epoxy resin from Resoltech (Resoltech 1050 and Hardener Resoltech 1058) was used for the embodiment of microcapsules after their fabrication and pre-impregnated (prepreg) carbon fiber from Hexcel was used to manufacture samples containing the healing system [11].

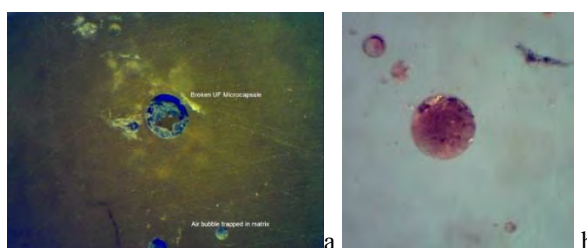
**Table 1. Chemicals used for the fabrication process of microcapsules [3]**

Name of the solution	Molecular formula	Physical description	Role in encapsulation process
Urea	CH <sub>4</sub> N <sub>2</sub> O	White crystalline powder Melting point: 135°C	Aqueous capsule wall formation
Resorcinol (1,3-benzenediol)	C <sub>6</sub> H <sub>4</sub> (OH) <sub>2</sub>	White needle crystals Melting point: 113°C	To make resin with formaldehyde
Formaldehyde	CH <sub>2</sub> O	Colorless liquid	Capsule wall formation
Dicyclopentadiene (DCPD)	C <sub>10</sub> H <sub>12</sub>	Colorless solid Melting point: 32.5°C	Monomer- Core of capsule
Ethylene Maleic Anhydride Copolymer (EMA)	C <sub>4</sub> H <sub>2</sub> O <sub>3</sub>	White powder	Additive emulsifier
Sodium Hydroxide	NaOH	White solid	Raise the pH of the solution
Hydrochloric acid	HCl	Aqueous solution, strong odour	Lower the solution pH level
Ammonium Chloride	NH <sub>4</sub> Cl	White powder	Hardener for formaldehyde

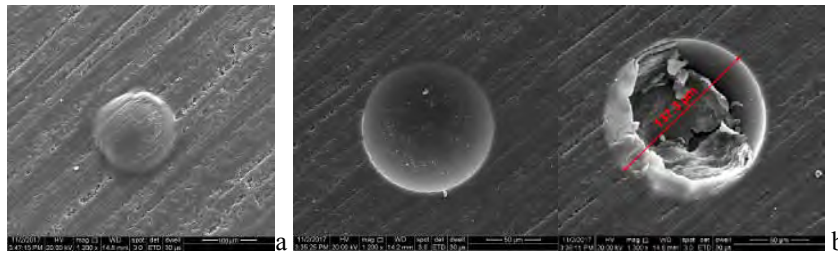
For the fabrication of microcapsules [11], a solution of 150mL water, 7g urea, 0.5g resorcinol and 0.5g ammonium chloride were introduced in a 600mL beaker and the mixture was placed on a magnetic hot plate where the agitation rate was increased to 600rpm at room temperature. The chemicals were in a solid state, so the mixture needed 10-15 minutes to homogenize, after which, 5%EMA copolymer was introduced in the solution. The solution pH was raised from 1.5 to 3.5 by the addition of NaOH and HCl. At this point the temperature was raised to 35°C. Because DCPD was in a solid state, it had to be melted prior adding it to the mixture. Therefore, 60g of DCPD were introduced in a 200mL beaker and placed on the hot plate, next to previously mentioned solution. When DCPD melted, it was introduced in the first solution. To the obtained emulsion, 18.91g of formaldehyde (37%) was added whilst the hotplate temperature was raised to 50°C, the agitation rate dropped to 500rpm and left for two hours. Agitation rate dictates the mean diameter of the microcapsules, thus with a higher agitation rate, a lower diameter is obtained. After 2 hours, 200mL of water had been introduced to the emulsion and left for another 2 hours, after which the emulsion was brought to room temperature and the microcapsules were separated. The microcapsule slurry was diluted with an additional 200mL of water and washed with water. The microcapsules were separated by vacuum filtration and left at room temperature for 48h to dry. The obtained microcapsules had a mean diameter between 100µm and 200µm. After the slurry of microcapsules was dried, they were investigated under OM and SEM before (Fig. 1) and after (Fig. 2) immersion in epoxy resin. For the embodiment of microcapsules in epoxy resin, 10mL resin (Resoltech 1050) and 3mL catalyst (Resoltech 1058) were used, having a mixture ratio of 100:30 and 10%mas. microcapsules. SEM images (Fig. 3) showed the cavities left by the microcapsules in the matrix as well as the surface morphology of the microcapsules [11].



**Fig. 1 OM images of obtained microcapsules [11]**



**Fig. 2 Microcapsules embedded in epoxy resin. a) broken microcapsule; b) full body microcapsule [11]**



**Fig. 3 SEM images of a) microcapsule embedded in resin and b) cavities left from microcapsule breakage [11]**

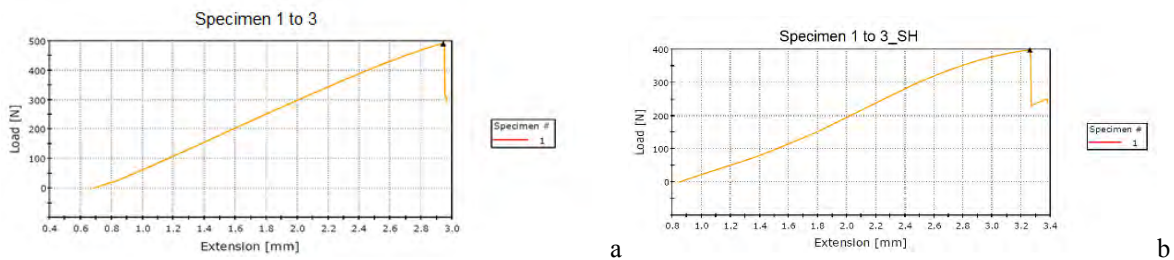
Composite samples having 100x15x2mm were prepared according to SR EN ISO 14125 (Class IV), using M49/42%/200T2X2/CHS-3K prepreg material from Hexcel. For their fabrication a multi-nest mould was used, as shown in Fig. 4. For each sample, a total of 8 plies having the dimension of 100x15 mm were needed, thus obtaining the two mm thickness. Each 8 ply set was weighted, then a 5%wt. Grubbs catalyst and 10%wt. microcapsules were weighted accordingly. The stacking sequence was as follows: [0°/0°/SH/0°/0°/SH/0°/0°], where SH represents the self-healing system. After the lay-up process, a layer of peel ply was placed on the multi-nest mould to retain the excess resin content during the curing process and over it, a layer of release film was placed to prevent the resin to flow within the vacuum bag. The vacuum bag was sealed with sealant tape and a vacuum connector was placed inside and connected to the oven. The curing cycle was set to 120°C for 2 hours with constant vacuum and no pressure. After the samples were removed from the mould, they were subjected to 3-point bending test (Fig. 5), with 2 mm/min speed rate. Samples containing healing system were tested until flexural break (Fig. 6), and the results showed a mean flexural strength value of 600,27 MPa with a 2.65 mm elongation. After the initial tests, they were left for 24 hours at 35 °C-40 °C for the healing system to take effect. After 24 hours, the samples were tested again, in the same conditions, showing a mean flexural strength value of 564,97 MPa with 3,29mm elongation (meaning a close 94%).



**Fig. 4 Multi-nest mould and the vacuum bag assembly for sample fabrication [11]**



**Fig. 5 Samples subjected to 3-point bend tests [11]**



**Fig. 6 Example of a sample a) at initial loading and b) second loading after 24 hours [8]**

### 3. CONCLUSIONS

UF microcapsules containing DCPD as healing agent were obtained, with dimensions ranging between 100µm si 200µm, due to 500rpm aggitation rate. Both OM and SEM investigation showed the formation of microcapsules along with their presence in the matrix. Cavities found in the matrix showed the neat, smooth exterior of the microcapsules before their rupture while samples preparation. A self-healing behaviour of fibre reinforced composite materials integrating dicyclopentadiene filled urea-formaldehyde microcapsules as healing system and Grubb's catalyst as reaction catalyst has been obtained. Flexural tests showed a healing efficiency of about 94% after 24 hours. Due to the fact that just few samples exhibited close values in recovering strength after 24hours, some additional investigations have to be performed with increasing the percentage of healing agents (20%wt. microcapsules) and an increase of temperature for the healing system to take effect (55°C-60°C curing for 24hours safter initial tests).

### ACKNOWLEDGEMENT

This work was carried out within "Nucleu" Program TURBO 2020, supported by the Romanian Minister of Research and Innovation, project number PN 16.26.04.05.

### REFERENCES

- [1] S.K. Ghosh, *Self-Healing Materials: Fundamentals, Design Strategies, and Applications*, Wiley-VCH Verlag GmbH & Co. KGaA, 2009, pp. 1.
- [2] G. Liberata, R. Marialuigia, N. Carlo, L. Pasquale, M. Annaluisa, H.B. Wolfgang, *Smart Mater. Struct.* 23 (2014) 045001.
- [3] L. Mercy, S. Prakash, *Characterisation of Dicyclopentadiene Filled Microcapsules for Self-Healing Composite Materials*, *Applied Mechanics and Materials Vols 766-767* (2015) pp 3-7
- [4] S.Vander Zwaag, (2007), *Self healing materials*, Springer publications.
- [5] R.E. Neisiany, J.K. Yoong Lee, S.N. Khorasani, R. Bagheri, S. Ramakrishna, Facile strategy toward fabrication of highly responsive self-healing carbon/epoxy composites via incorporation of healing agents encapsulated in poly(methylmethacrylate) nanofiber shell, *Journal of Industrial and Engineering Chemistry*, 2017
- [6] F. Ahangaran, M. Hayaty, A.H. Navarchian, Morphological study of polymethyl methacrylate microcapsules filled with self-healing agents, *Applied Surface Science* 399 (2017) 721–731.
- [7] R.S. Neisiany, J.K. Yoong Lee, S.N. Khorasani, S. Ramakrishna, Towards the development of self-healing carbon/epoxy composites with improved potential provided by efficient encapsulation of healing agents in core-shell nanofibers, *Polymer Testing* 62 (2017) 79-87
- [8] R. Luterbacher, T.S. Coope, R.S. Trask, I.P. Bond, Vascular self-healing within carbon fibre reinforced polymer stringer run-out configurations, *Composites Science and Technology* 136 (2016) 67-75
- [9] S. Saini, D. Jain, The effect of healing time on the self-healing efficiency of carbon fibre reinforced polymer composites, 5th International Conference on Materials Processing and Characterization, *Materials Today: Proceedings* 4 (2017) 2903–2909
- [10] S.R. White, N.R. Sottos, P.H. Geubelle, J.S. Moore, M.R. Kessler, S.R. Sriram, E.N. Brown, S. Viswanathan (2001), Autonomic healing of Polymeric composites, *Nature*, Vol.409, pp. 794-797.
- [11] S. Vintila, R. Condruz, A. Paraschiv, Characterization of self-healing performances on frp composites, Workshop On Smart Specialization And Advanced Materials For Extreme Conditions SUPERAMT, Nov. 20-22, 2017, Bucharest, Romania

# EVALUATION OF MECHANICAL PROPERTIES OF CARBON NANOTUBE REINFORCED COMPOSITES

Mihaela Raluca CONDRUZ<sup>4</sup>, Sebastian Ionuț VINTILĂ<sup>4</sup>, Alexandru PARASCHIV<sup>4</sup>

**ABSTRACT:** The present research was focused on evaluation of multi-wall carbon nanotubes influence on ordinary polymeric composites, starting with integration of the nanotubes, optical microscopic analysis, mechanical testing to determine flexural properties of epoxy nanocomposites and hybrid composites and thermal analysis of hybrid composites. It was observed that changes in the manufacturing process parameters can influence the properties of nanocomposites. A reduction in the elasticity of the epoxy matrix was observed after the addition of carbon nanotubes. Also, it was established that even if the nanotubes are functionalized with -COOH group they still present the tendency to form bundles, leading to more rapid failure of the material. The addition of carbon nanotubes between the prepreg plies oriented at 0° leads to a reduction of material's mechanical properties, while in case of hybrid composites with prepreg plies oriented at 45° an increase of material's mechanical properties was observed. Regarding the thermal analysis, a slight modification of the hybrid material's Tg was observed (an increase of 1%).

**KEYWORDS:** nanocomposites, hybrid composites, three point bending, polymers

## 1. INTRODUCTION

The material scientists are continuously searching for new ways to improve material properties and to develop new materials. A solution to attain such goals is to integrate nanomaterials in different organic components such as polymers to provide a synergistic improvement in properties when the component sizes are at nano level [1]. The present study is focused on the integration of multi-wall carbon nanotubes (MWCNT) in organic polymers and organic polymeric composites. In plenty literature reviews can be found the advantages of integrating carbon nanotubes in organic polymers, they can ensure improvement of material's conductivity, strength, flexibility/flowability, thermal stability/flame retardancy, simultaneous with keeping the overall low weight [1 - 4]. A problem encountered in case of CNTs is their tendency to agglomerate into bundles due to van der Waals forces. To avoid this problem several methods were developed (using organic solvents, selecting a suitable dispersion method and optimum process parameters, surface functionalization) [5]. The present research goal was to evaluate the influence of f-MWCNT (functionalized multi-wall carbon nanotube) addition on epoxy resin and on hybrid polymeric composites. To achieve this goal, several investigations were performed: SEM analysis on MWCNTs, evaluation of different manufacturing process parameters, optical microscopy on manufactured nanocomposites, thermal analysis (differential scanning calorimetry – DSC) on hybrid composites, mechanical testing (three point bending) of all composite samples.

## 2. EXPERIMENTAL APPROACH

### 2.1. Materials and procedures

For this investigation, two types of polymeric composites were manufactured along with corresponding references for each material configuration:

---

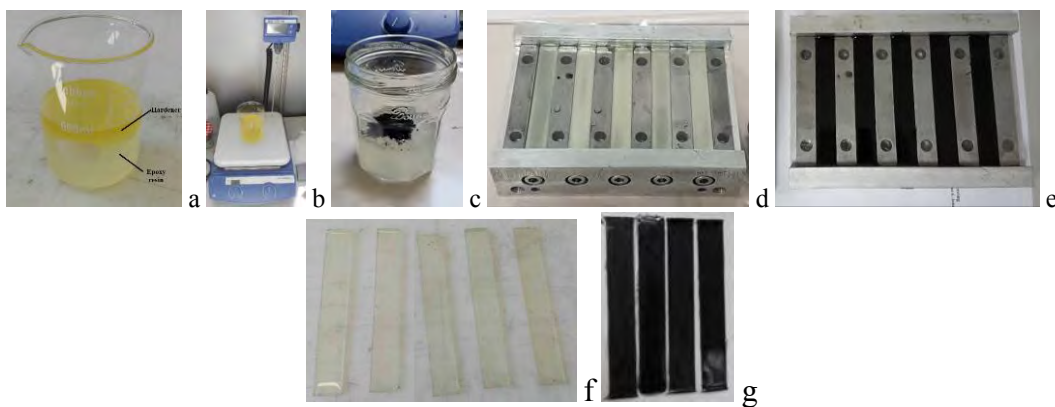
<sup>4</sup> Romanian Research and Development Institute for Gas Turbines - COMOTI

- Nanocomposites reinforced with MWCNT along with neat epoxy references;
- Hybrid composites reinforced with carbon fiber fabrics which integrate MWCNT between prepreg plies oriented at 0° or at 45° along with prepreg based references manufactured without MWCNT.

*Nanocomposite manufacturing process*

To manufacture nanocomposites three precursors were used: an epoxy system consisting in epoxy resin (Resoltech 1050) and hardener (Resoltech 1058), and as nanoreinforcement -COOH f-MWCNT.

The influence of different manufacturing process parameters on mechanical properties were evaluated. Thus 0,25%wt. MWCNT were integrated in the epoxy resin by magnetic stirring using two different homogenization parameters to obtain two sample batches. In case of the first sample batch the rotational speed of the magnet was 1500 rot./min. for 1,5 hours, then the hardener was added and the solution was stirred for another 5 minutes. In case of the second sample batch, the rotational speed was 800 rot./min. for 3 hours, then the hardener was added and stirred for another 5 minutes. The mixtures were cast into multi-nest moulds and were cured at ambient temperature (25±5°C) for one week. The manufacturing process of reference and nanocomposite samples is presented in Fig. 1.

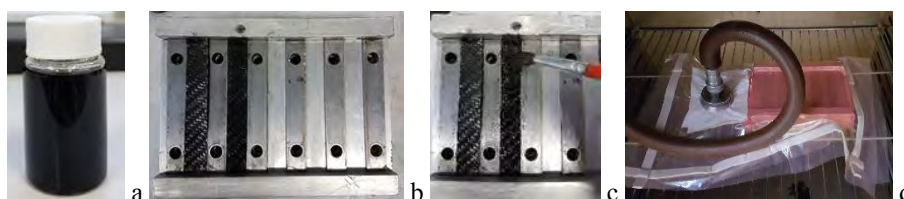


**Fig. 1 Manufacturing of nanocomposite samples and corresponding references: a) the epoxy system; b) homogenization of the epoxy system; c) f-MWCNT addition on epoxy resin; d) reference samples in multi-nest mould; e) nanocomposite samples in multi-nest mould; f, g) cured samples**

*Hybrid composite manufacturing process*

For the manufacturing of hybrid composites, an epoxy prepreg precursor was selected. It consisted in a twill 2x2 carbon fiber fabric with 42% resin content (HexPly M49/42%/200T2X2/CHS-3K provided by Hexcel). In this case, the influence of different ply orientation (0° and 45°) was analysed as well as the nanoreinforcement integration influence on the mechanical and thermal properties of hybrid composites.

The references for hybrid composites consisted in neat prepreg samples, while hybrid composites consisted in prepreg samples with f-MWCNT between each prepreg ply. For each configuration 8 plies of prepreg were used. A f-MWCNT suspension was prepared using the magnetic stirrer and methanol. The f-MWCNT suspension was integrated between each ply by hand lay-up using a brush, leaving the methanol to evaporate at ambient temperature. The same multi-nest mould was used to manufacture the hybrid composite samples and corresponding references. A vacuum bag ensemble was realised and it was introduced in a vacuum assisted oven for curing. To cure the samples, the oven was heated from 20°C until 120°C (heating rate of ~3°C/min.), afterwards the samples were hold for 2 hours at 120°C and then were oven assisted cooled. The manufacturing process of hybrid samples is showed in Fig. 2.



**Fig. 2 Manufacturing of hybrid composite samples: a) f-MWCNT suspension; b, c) preparation of hybrid samples; d) vacuum ensemble in the oven connected to the vacuum pump**

In this study, different investigations were performed to characterize the material properties. Firstly, a SEM analysis was performed on the f-MWCNT using FEI Inspect F50 electronic microscope. The goal of the investigation was to observe the nanotubes form and surface. Also, a dimensional analysis was performed on the f-MWCNT using Scandium image processing software. Due to the fact that the obtained nanocomposite samples are translucent, an optic microscopy analysis was considered appropriate to observe the distribution of carbon nanotubes in the epoxy matrix.

As it was found in the literature [6], carbon nanotubes can influence the glass transition temperature ( $T_g$ ) of polymers. The influence of f-MWCNT on  $T_g$  was evaluated by thermal analysis performed with DSC 8000. DSC analysis was performed on a reference sample made of 4 prepreg plies and a hybrid sample integrating f-MWCNT between each ply. The method used consisted in sample maintaining at  $30^\circ\text{C}$  for 1 min. then heating until  $200^\circ\text{C}$  for 34 min., afterwards the DSC oven was rapidly cooled until  $30^\circ\text{C}$ .

Three point bending tests were performed on 5 samples of each configuration using a mechanical testing machine Instron 3360 (static load cell of 50 kN). For mechanical tests, SR EN ISO 14125:2000 [7] was consulted, thereby displacement was 2 mm./min, and the distance between the supports was 32 mm.

### 2.2. Results and discussions

The SEM analysis showed that MWCNTs present a tubular shape and a rugged surface (this could be a result of the functionalization of the nanotube surface) and they are disposed into bundles (Fig. 3 a). The dimensional analysis showed that the majority of the MWCNT's diameter is in the range of 20-30 nm.

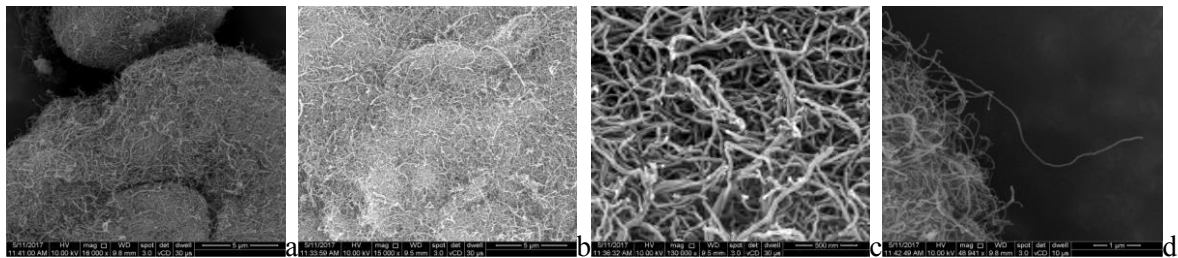


Fig. 3 a,b,c,d) SEM images with f-MWCNT used as reinforcing agent

Three point tests were performed on all sample configuration (each sample batch consisted in 5 samples). Fig. 4 and Fig. 5 show images during the mechanical testing of nanocomposite and hybrid samples and the average values of the mechanical properties obtained are summarized in Table 1. Fig. 6 shows representative results of three point bending tests. Fig. 6 a) presents three representative stress – strain curves of the epoxy system along with 1<sup>st</sup> and 2<sup>nd</sup> nanocomposite sample batch while Fig. 6 b) presents representative results for the mechanical tests of hybrid composites with  $0^\circ$  ply orientation. Fig. 6 c) shows representative results for the tests performed on hybrid composites with  $45^\circ$  ply orientation.

It was observed that the manufacturing process parameters (rotational speed, homogenization time) influenced the mechanical properties of the material due to the dispersion degree of the nanotubes in the epoxy matrix. A more homogenous dispersion observed in case of the 2<sup>nd</sup> sample batch ensured the increase of mechanical properties of the nanomaterial compared with the 1<sup>st</sup> sample batch. The 1<sup>st</sup> homogenization process parameters didn't ensure a high homogenous distribution of the nanotubes, they had the tendency to form bundles which represent areas that induce high internal stresses in the material and have the same behaviour as a fracture inducer. Unlike the 1<sup>st</sup> homogenization process parameters, the 2<sup>nd</sup> process parameters ensure a higher homogeneity resulting in higher mechanical properties. These observations are supported by the optic microscopy analysis (Fig. 7, Fig. 8).

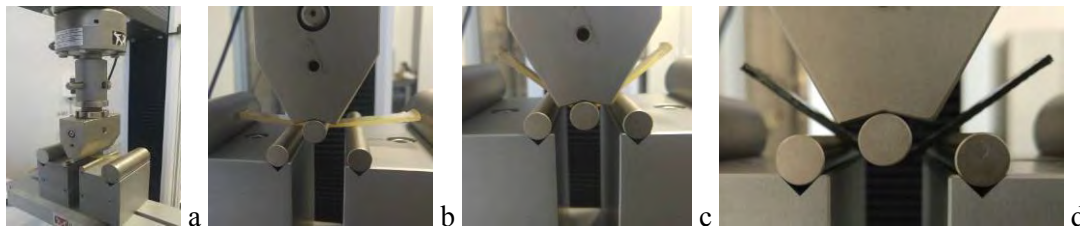


Fig. 4 Images with nanocomposite samples and corresponding references during three point bending

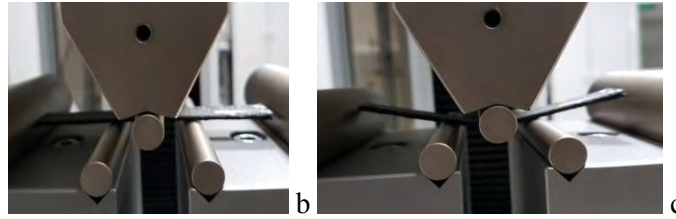


Fig. 5 Images with hybrid composite samples during three point bending tests

Table 1. Mechanical test results obtained for composite samples

Samples	Load at tensile strength [N]	Flexure stress at maximum load [MPa]	Load at break [N]
<b>Nanocomposite reference</b>	<b>193</b>	<b>75</b>	<b>10</b>
Nanocomposite first sample batch	75	41,7	9,8
Nanocomposite second sample batch	115	63,5	10,8
<b>Hybrid composite reference with orientation ply at 0°</b>	<b>620</b>	<b>499</b>	<b>311</b>
Hybrid composite with orientation ply at 0°	548	472	278
<b>Hybrid composite reference with orientation ply at 45°</b>	<b>277</b>	<b>234</b>	<b>237</b>
Hybrid composite with orientation ply at 45°	303	250	236

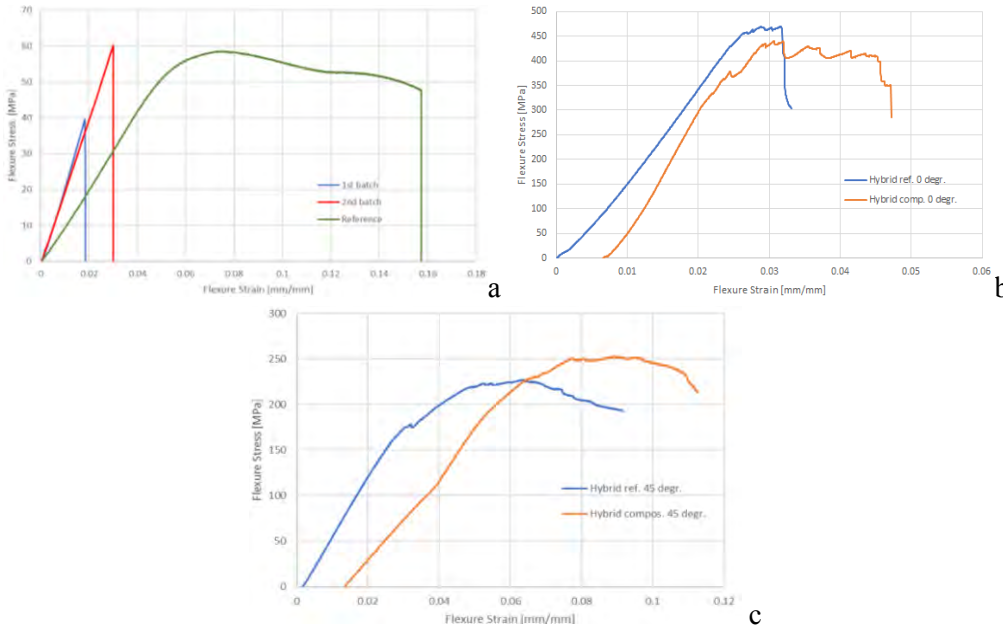


Fig. 6 Graphic representation of stress – strain curves of nanocomposites and hybrid composites – representative three point bending results

MWCNT addition reduces the elasticity of epoxy while increases the material stiffness. Mechanical test results showed that in case of the 1<sup>st</sup> sample batch the distribution of MWCNT resulted in 45% reduction of mechanical resistance, while in case of the 2<sup>nd</sup> sample batch the distribution of MWCNT was more homogenous, reducing the mechanical properties only with 15% compared with the references. Thereby, even if the mechanical properties were reduced in case of the 2<sup>nd</sup> sample batch, they showed a slightly increase compared with the 1<sup>st</sup> sample batch.

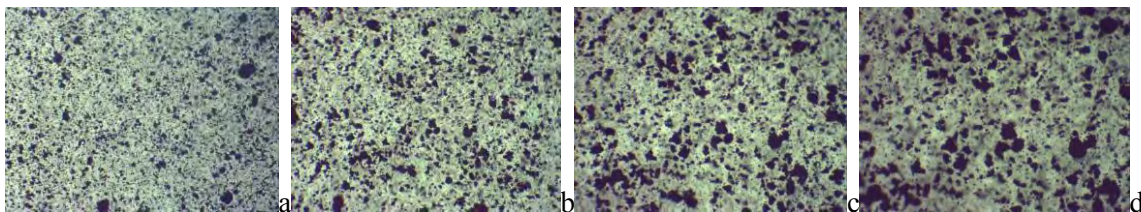


Fig. 7 Optic microscopy images with 1<sup>st</sup> sample batch of nanocomposites at different magnifications



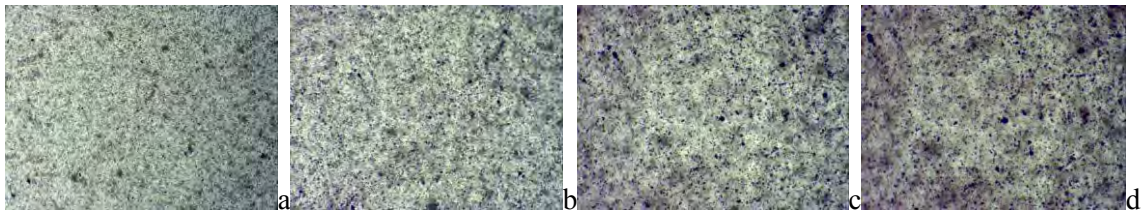


Fig. 8 Optic microscopy images with 2<sup>nd</sup> sample batch of nanocomposites at different magnifications

Regarding three point bending results of hybrid composites with prepreg plies orientated at 0° it was observed a reduction of 12% of the maximum load at tensile strength, a reduction of 5% of flexure stress la maximum load and a reduction of 10% of load at break compared with the prepreg references. The reduction of properties can be caused by the preferential distribution of MWCNT during the lay-up with the brush, or during the curing cycle when the resin “softens” and the excess is absorbed by the auxiliary materials of the vacuum bag.

Regarding three point bending results of hybrid composites with prepreg plies orientated at 45° it was observed an increase with 10% of load at tensile strength and an increase of 7% of the flexure stress at maximum load. In this case even if the carbon nanotubes form bundles during lay-up, their presence has a positive influence on the composite, ensuring a better support on transverse direction of the carbon fibres.

The DSC analysis showed that the resin used for the prepreg is a crystalline polymer, in the thermograms presented in Fig. 9 can be observed a pick corresponding to a exotherm reaction for a crystalline polymer.

The reference sample presents a crystallization temperature  $T_c = 152,45^\circ\text{C}$  and a  $T_g = 146,28^\circ\text{C}$ , while the hybrid composite sample presents a crystallization temperature  $T_c = 153,28^\circ\text{C}$  and a  $T_g = 148,46^\circ\text{C}$ . A slight modification of the  $T_g$  was observed (an increase of 1% in case of the hybrid composite).

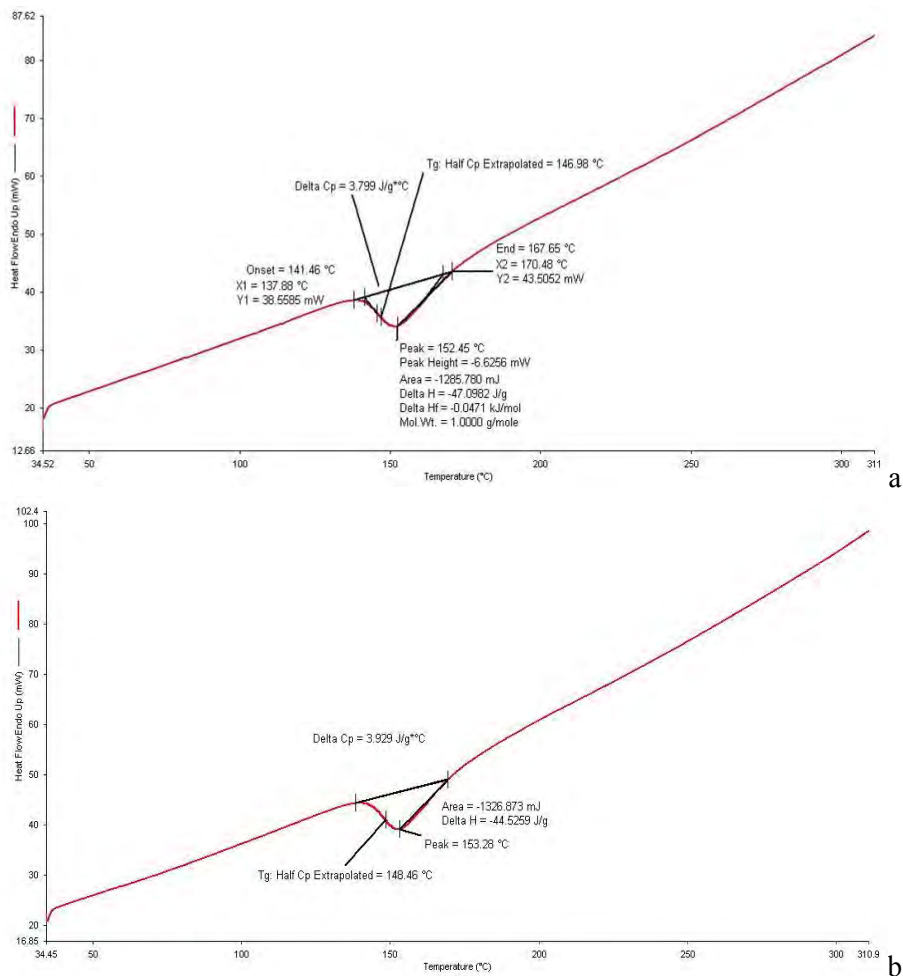


Fig. 9 Thermograms with: a) reference sample results; b) hybrid composite sample results

### 3. CONCLUSIONS

The goal of present research was to evaluate the influence of different manufacturing parameters, orientation of plies and addition of carbon nanotubes on polymeric composites properties. To ensure the achievement of the research goal two categories of polymeric composites: polymeric nanocomposites (epoxy system reinforced with f-MWCNT) and hybrid composites (epoxy prepreg integrating f-MWCNT between each plies). A SEM analysis was performed on the f-MWCNT used as reinforcement to characterise the nanotubes and an optic microscopy analysis was performed to evaluate the distribution of carbon nanotubes in the epoxy matrix. Also, a DSC analysis was performed on the hybrid composites to determine the influence of the f-MWCNT on the T<sub>g</sub> value along with a three point bending test campaign.

It was observed that changes in the manufacturing parameters can influence the properties of the nanocomposites, a homogenous distribution of the nanotubes in the epoxy matrix can increase the flexure properties of the nanocomposites. Additional studies have to be performed regarding the optimum parameters of nanotubes integration in epoxy resin, a solution has to be found to reduce the bundle of nanotubes.

A reduction in the elasticity of the epoxy matrix was observed after the addition of f-MWCNT, moreover the tendency of the nanotubes to agglomerate leads to rapid failure of the material.

In case of hybrid composite materials with prepreg plies oriented at 0°, by adding f-MWCNT was observed a reduction of mechanical properties, while in case of hybrid composites with prepreg plies oriented at 45° an increase of mechanical properties was observed. Regarding the DSC analysis, a slight modification of the T<sub>g</sub> of the hybrid material was observed (an increase of 1%), fact that was found also in the literature.

The novelty of this research consisted in the fact that an increase of mechanical properties was observed for hybrid composites even if the nanotubes were bundled. In case of using prepreg plies oriented at 45°, the nanotubes act as an additional reinforcement (the hybrid resulted consisting in a 3D reinforced polymer).

### ACKNOWLEDGEMENT

This work was carried out within “Nucleu” Program TURBO 2020, supported by the Romanian Minister of Research and Innovation, project number PN 16.26.04.04.

### REFERENCES

- [1] D. Ratna; 2005; Nanoreinforcement of Epoxy; *Epoxy Composites: Impact Resistance and Flame Retardancy*; Vol. 16; No. 5; Rapra Technology; United Kingdom; 17 - 21
- [2] C. Kingston, R. Zepp, A. Andrady, D. Boverhof, R. Fehir, D. Howkins, J. Roberts, P. Sayre, B. Shelton, Y. Sultan, V. Vejins, W. Wohlleben; 2014; Release characteristics of selected carbon nanotube polymer composites, *Carbon*; 68, 33-57
- [3] T. Hayashi, M. Endo; 2011; Carbon nanotubes as structural material and their application in composites; *Composites: Part B*, 42, 2151-2517
- [4] M.R. Condruz, I.S. Vintila; 2017; Carbon nanotube and nanoclay based polymeric composites – recent achievements and future development directions; *Scientific Journal TURBO, IV* (1), 19-22
- [5] R. Atif, F. Inam; 2016; Reasons and remedies for the agglomeration of multi-layered graphene and carbon nanotubes in polymers; *Beilstein J. Nanotechnol.*; 7, 1174-1196
- [6] A. Allaoi, N. El Bounia; 2009; How carbon nanotubes affect the cure kinetics and glass transition temperature of their epoxy composites? *eXPRESS Polymer Letters*; 3 (9); 588-594
- [7] SR EN ISO 14125:2000 Fibre-reinforced plastic composites. Determination of flexural properties

# NUMERICAL INVESTIGATION OF A SCREW COMPRESSOR PERFORMANCE

Ion MĂLĂEL<sup>5</sup>, Mihail SIMA<sup>5</sup>

**ABSTRACT:** In this paper the CHP 220 screw compressor performance evaluation was performed by using the numerical methods. Thus, for the CFD analysis has defined the computing domain comprised of two sub-domains, one rotational and one stationary. The TwinMesh software, dedicated to volumetric machines with positive displacement, was used for the meshing of the rotors. The SST turbulence model has been used for flow modelling. Also, the finite element analysis of the stress and deformation state in the screw compressor rotors was performed. As inputs to FEM analysis, the results of the CFD analysis, performed on the working environment, were used. Finally, the results consist of the variation of the absolute pressure from the inlet to the compressor outlet, the variation of the massflow, the distribution of the sealing fluid (oil), but also the distributions of the stress tensor and the displacements together with the safety coefficients.

**KEYWORDS:** screw compressor, CFD, FEM, TwinMesh, volumetric machine

## NOMENCLATURE

*All variables are defined throughout the work.*

## 1. INTRODUCTION

The screw compressors are volumetric machines with positive displacement that can be used in refrigeration and air conditioning but also in power generation. Even though the concept of screw compressor is relatively new, studies have been developed on thermodynamics of screw compressors in order to obtain a calculation model. These models were used both for performance evaluation and optimization of rotor lobe profiles. Among the best-known models are those made by Bein and Hamilton [1], Boblitt and Moore [2], Jianhua and Guangxi [3]

CFD (Computational Fluid Dynamics) methods can be used to predict the performance of such machine. The use of these methods in studying flow in screw compressors involves studies of non-stationary flow with movement boundaries. Flows with such boundary were also developed by Peric [4], Demirdzic and Peric [5], and Demirdzic and Muzaferija [6].

When using finite volume methods in studying screw compressor flow, a particularly important problem, namely generating the calculation grid for unsteady simulations with grid movements, appears. As the volumes in the compressor change as the rotors rotate, the calculation grid must be deformed. At present, no commercial computing grid is able to do so, as Kovacevic [7] and Prasad [8] have shown in their works.

Despite the above, there are only a few reports on unsteady flow in 3D for screw compressors with high discharge pressures.

Increasing the storage capacity of natural gas is one of the directions of action adopted by the main energy suppliers. Achieving the objectives following this action line requires the development of compression capabilities with direct implications in increasing the working pressure of the compressors. In this regard, the design of a screw compressor to provide a high flow rate at a considerable discharge pressure implies the evaluation of the mechanical strength of the compressor parts, given that the compressor standards provide a test sample of the assembly at a pressure of 1,5 times the discharge pressure. The rigidity evaluation will be

---

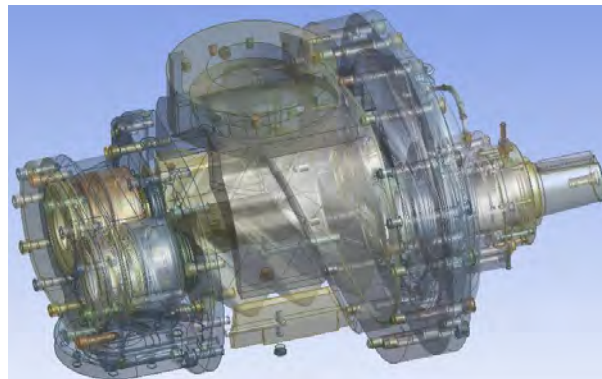
<sup>5</sup> National Research and Development Institute for Gas Turbines COMOTI, Bucharest, Romania

done by calculating the deformations generated by the pressure and distribution of the thermal field on the rotors.

In this study, the CHP 220 screw compressor having a suction pressure of 4.5 bar and 30 bar at discharge.

## 2. PAPER CONTENTS

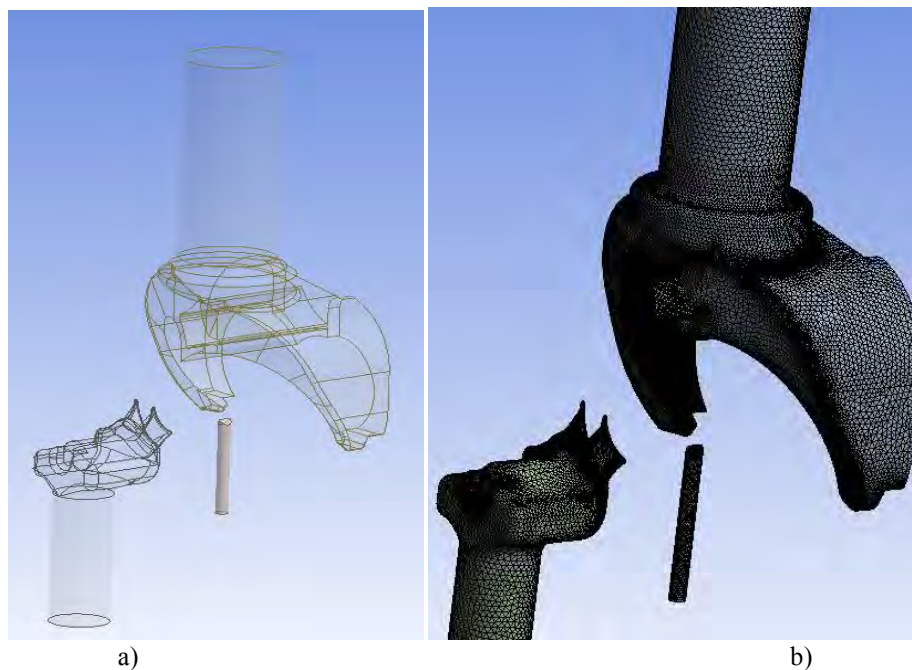
By using the CHP 220 screw compressor geometry, we have defined the computational domain for this study. Figure 1 shows the geometry of the screw compressor used in numerical analysis.



**Fig. 1. The CHP 220 screw compressor geometry**

Starting from the 3D CAD model, the computational domain for the stator component of the screw compressor, which is composed of three subdomains, has been defined: the suction sub-domain, the oil input sub-domain, and the sub-domain of the discharge. Boolean functions for subtraction and union were used to define the domains. In figure 2 a) are represented the three subdomains made using the Ansys Design Modeler software.

The mesh (Figure 2b) for the stator component was generated with Ansys Meshing, where meshing methods were used based on the surface size and volume size of the element. Figure 3 shows the surfaces for the boundary conditions and a cross section of this mesh.



**Fig 2. a) Computational domain for the stator parts; b) The mesh for stator parts**

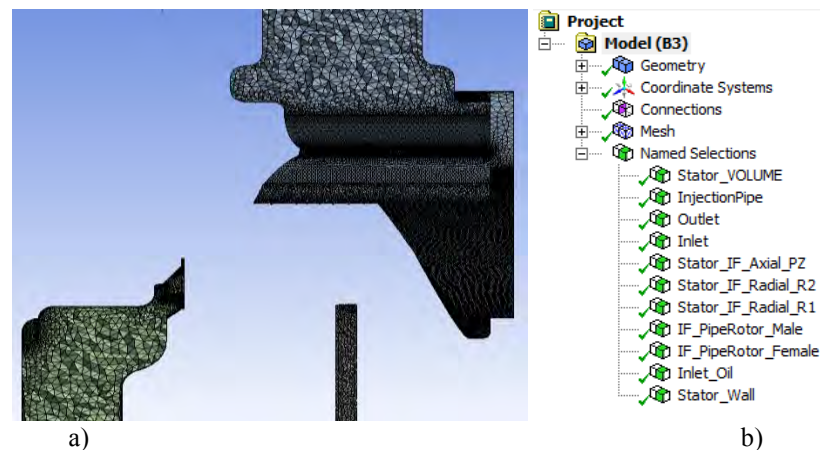


Fig. 3. a) Cross section thru the mesh; b) Surfaces selection for BC

For the rotor domain, the commercial software for volumetric machines with positive displacement, TwinMesh, was used. Figure 4 shows the 2D grid and its quality.

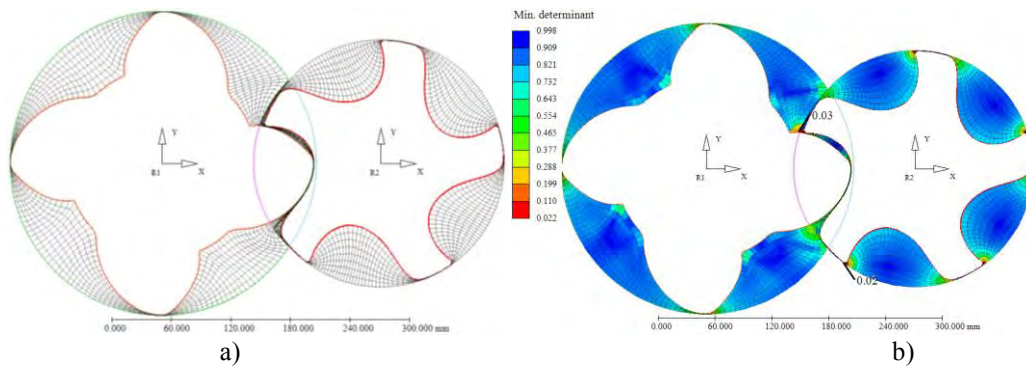
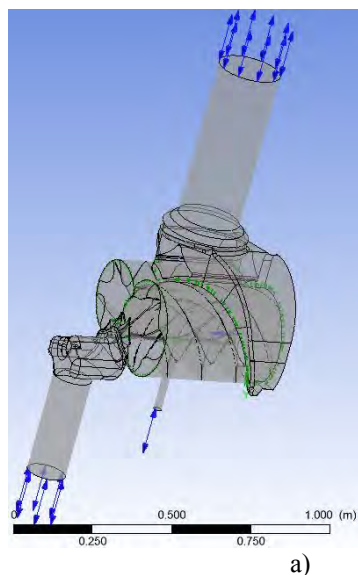


Fig 4. a) 2D mesh; b) Mesh quality

Figure 5 shows the boundary conditions defined in Ansys CFX Pre together with the list of expert parameters used for solution stability. For this analysis, the SST turbulence model was used. As boundary conditions were used opening conditions where the pressure value was imposed. For the outlet a function for increasing the pressure has been defined.



```

FLOW: Flow Analysis 1
&replace EXPERT PARAMETERS:
  backup file at zero = t
  compressible linearisation option = 3
  max solver its fluids = 80
  min solver its fluids = 40
  multigrid solver = f
  outer loop relaxations default = 0.1
  solver relaxation fluids = 0.8
  solver target reduction fluids = 0.05
  stationary interface reintersection = f
  topology estimate factor = 1.2
  topology estimate factor zif = 1.2
END
END
    
```

Fig 5. a) BC; b) Expert parameters from ANSYS CFX pre

In the figure 6 is represented the absolute pressure from the compressor. The blue color is the suction pressure value, 4.5 bar, and the red color is the discharge pressure that is 30 bar. Using the "opening" boundary conditions with the required pressure, both the massflow variation (Figure 7a) and the variation of the oil flow at the compressor inlet (Figure 7b) were determined. Also the power variation for a complete 360 degree rotation was determined (Figure 8).

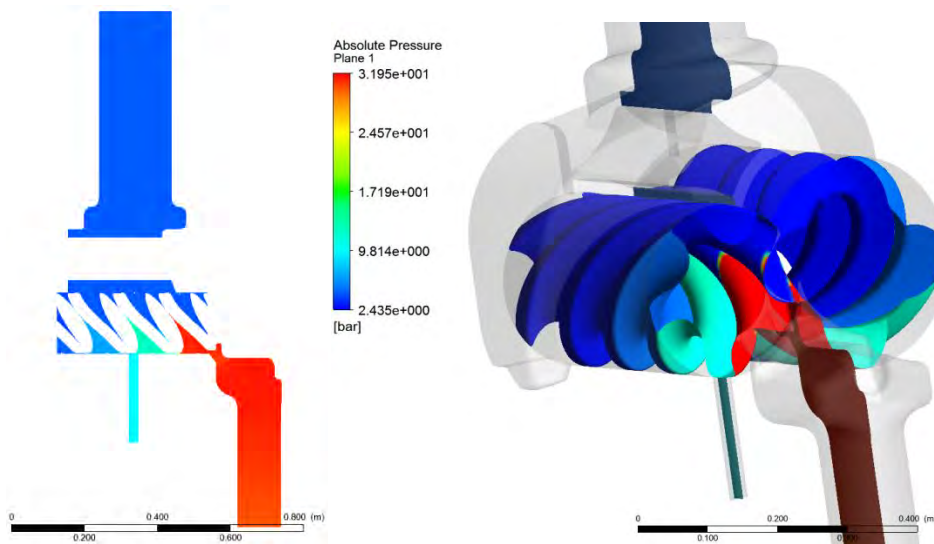


Fig 6. Absolute pressure

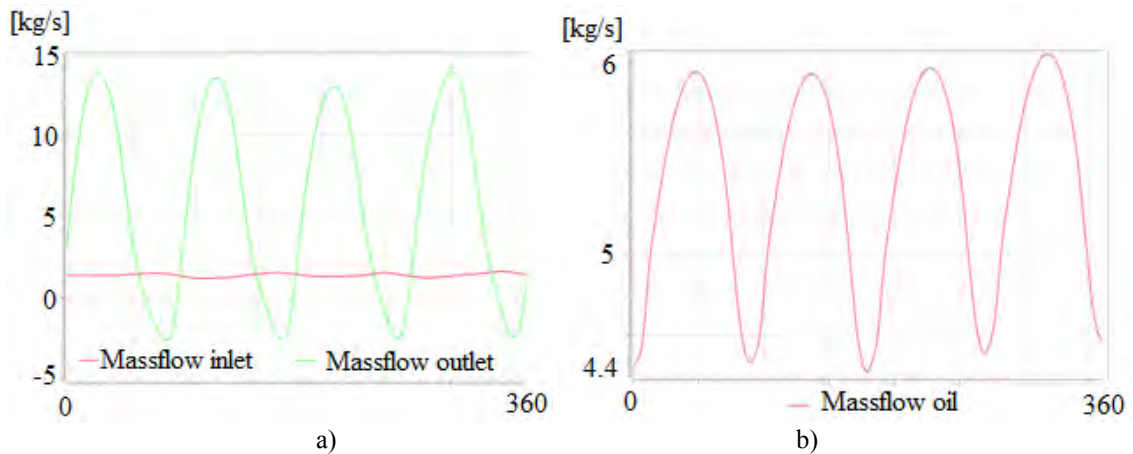


Fig 7. a) Air massflow; b) Oil massflow

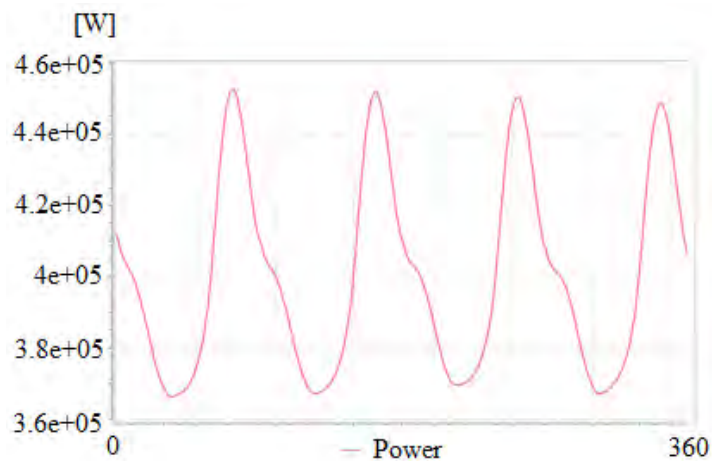


Fig 8. Power variation

For FEM analysis the following conditions were used: - inlet pressure of 0.45 MPa; - discharge pressure of 3.0 MPa; - maximum working pressure 4,1 MPa, and the mechanical properties of the material were as follows: elastic modulus:  $E = 1.68E11 \text{ N / mm}^2$ ; Poisson's coefficient:  $\nu = 0.28$ ; density  $\rho = 7860 \text{ kg / m}^3$ ; yield limit:  $\sigma_Y = 275 \text{ MPa}$ ; break elongation:  $\epsilon_r = 22\%$ ; ultimate stress:  $\sigma_U = 475 \text{ MPa}$ .

The Von Misses stress for both, male and female rotor is presented in figure 9 and the displacements in figure 10.

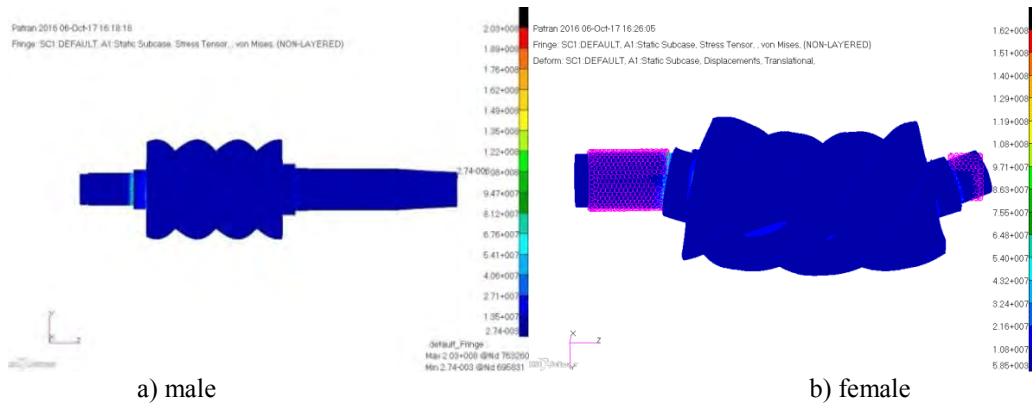


Fig 9. The Von Misses stress

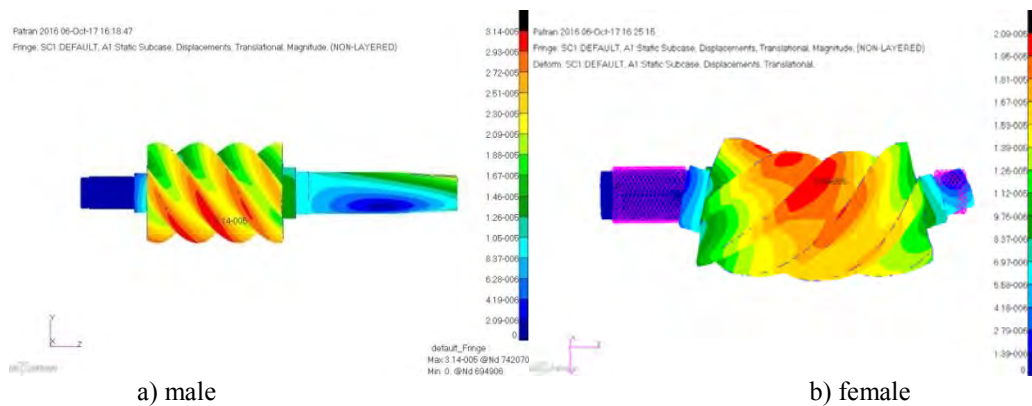


Fig 10. Rotors displacements

### 3. CONCLUSIONS

Numerical performance of a screw compressor using numerical methods was evaluated in this paper. For this study the geometry of the CHP 220 screw compressor has been used, which has a pressure of 4.5 bar at the inlet and a discharge pressure of 30 bar. Using the CFD Ansys CFX commercial software, variations in both gas and oil flow were determined.

The following Von Misses stresses were obtained by applying the CFD analysis pressures: female rotor: 163 MPa, safety coefficient 5 and for male: 203 MPa, safety coefficient 4 (yield limit is 800 MPa). Maximum rotors displacements are 21  $\mu\text{m}$  for the female and 31  $\mu\text{m}$  for the male (the clearance between the rotor is 40  $\mu\text{m}$  and between the rotors and case are 100  $\mu\text{m}$ ).

For future research, numerical data checks will be carried out using the experimental tests carried out on the test bench of INCDT COMOTI.

### ACKNOWLEDGEMENT

This work was carried out within “Nucleu” Program TURBO 2020, supported by the Romanian Minister of Research and Innovation, project number PN 16.26.06.07.

## REFERENCES

- [1] Bein, T.W., Hamilton, J.F., 1982. Computer modeling of an oil flooded single screw compressor. In: Proc Int Compressor Conf at Purdue. Paper 383.
- [2] Boblitt, W.W., Moore, J., 1984. Computer modeling of single-screw oil flooded refrigerant compressors. In: Proc. Int. Compressor Conf. at Purdue. Paper 506.
- [3] Jianhua, Wu, Guangxi, Jin, 1988. The computer simulation of oilflooded single screw compressors. In: Proc. Int. Compressor Conf. at Purdue. Paper 646.
- [4] Peric, M., 1985. A Finite Volume Method for the Prediction of Three Dimensional Fluid Flow in Complex Ducts (PhD thesis). Imperial College of Science, Technology & Medicine, London.
- [5] Demirdzic, I., Peric, M., 1990. Finite volume method for prediction of fluid flow in arbitrary shaped domains with moving boundaries. Int. J. Numer. Methods Fluids 10, 771.
- [6] Demirdzic, I., Muzaferija, S., 1995. Numerical method for coupled fluid flow, heat transfer and stress analysis using unstructured moving mesh with cells of arbitrary topology. Comp. Methods Appl. Mech. Eng. 125, 235e255.
- [7] Kovacevic, A., Stosic, N., Smith, I.K., 1999. Development of CADCFD interface for screw compressor design. In: International Conference on Compressors and their Systems, London, IMechE Proceedings, pp. 757e767. Paper C542-075
- [8] Prasad, B. G. Shiva, 2004. CFD for positive displacement compressors. In: Proc. Int. Compressor Conf. at Purdue. Paper 1689.
- [9] API 694 „Rotary-Type Positive-Displacement Compressors for Petroleum, Petrochemical, and Natural Gas Industries”, 4th edition, 2004;
- [10] Constantin, V., Palade, V. – Organe de masini și mecanisme, vol.I, Galați, Editura Fundației Universitare „Dunărea de Jos”, Galați, 2005;
- [11] N Stosic, E. Mujic and I K Smith - The Design of a High Efficiency Oil Flooded Gas Screw Compressor, City University London, November 2009;



## SCREW EXPANDER TESTED ON COMOTI BENCH AND AT BENEFICIARY

Valentin PETRESCU<sup>6</sup>, Niculae TOMA<sup>6</sup>, Cristian SLUJITORU<sup>6</sup>

**ABSTRACT:** National Research & Development Institute for Gas Turbines Comoti has developed a helical screw expander - asynchronous electric generator assembly – as well as a test system for tracking the parameters of thermal, mechanical and electrical processes during common or transitory working regimes, their adjustment and control in order to ensure maximum security working conditions. The element of novelty of this electric energy providing assembly constitutes the use of a helical turbine that works at lower speed than other classical expanders due to the elimination of the reductor which ensures the connection of the expander to the electric generator. The monitoring system introduces functional check-ups of the manual and electrical operated elements as well as the check-up of measuring lines of the analog parameters. The testing was done in the testing bench at COMOTI premises and it used air as a working agent. The results thus obtained constitute the preliminary data that may offer the possibility of placing the screw expander - electric generator assembly inside regulating and measurement stations.

**KEYWORDS:** energetic efficiency, clean energy, helical expander.

### 1. INTRODUCTION

To reduce the gas pressure in the regulating and measurement stations from the national piping network (with pressure up to 40 bara), lamination valves are used, usually heated to reduce the pressure from the national piping network to the local piping network. This leads to a significant loss of "green" energy that can be recovered through the efficient use of the differential pressure in the expander. The aim is to replace the rolling valves and regulators with a screw turbine which, by adiabatic expansion of gases produces a clean and usable energy. COMOTI developed an efficient equipment, a power conversion equipment that converts gas expansion in green electricity. This unique group works using oil-injected screw technology [1].

Natural gas (NG) is a major fossil fuel contributing to about one fourth of the world's primary energy consumption (23.8%). The fuel is transported to large distances by means of pipeline systems with compressor stations consuming between 3% and 5% of the chemical energy of the transported gas, depending on the distance covered. Alternatively, the gas can be transported as LNG (liquefied natural gas), which is bound to an energy cost of about 2.5% of LHV (lower heating value) for the liquefaction and a boil-off loss of 2–5% in the transport and storage chain [2].

While the LNG transport dominates the overseas trading, the pipeline transport is fundamental for inland transmission and distribution. The pipeline networks are organized hierarchically within 3–4 pressure stages, connected by pressure reduction stations (PRSs). In most PRSs, pressure reduction is performed in a pressure regulator, i.e. an automatically operated throttling valve. This solution ensures the reliability of supply, but destroys the available energy of pressurized gas which could be used to generate mechanical work as a result of the expansion process. Moreover, in order to prevent hydrate formation due to the temperature drop in the throttling process, the majority of PRS consume energy for gas pre-heating in order to maintain its temperature above the 'permissible safe temperature'; detailed regulations may further specify the limit value (e.g. 5–8 °C). As a result, the process of pressure reduction is energy consuming instead of being a source of energy generation [2]. It is technically possible to convert the available decrease in physical energy into mechanical

---

<sup>6</sup> National Research and Development Institute for Gas Turbines COMOTI, Bucharest, Romania

work by means of a piston, screw or a turbine expander (turboexpander). The generated work may be converted to electricity, some authors also suggested its direct application for hydrogen production or, in particular industrial applications, to drive compressors. Suitable expander technology is offered by many manufacturers worldwide [2].

The key problem limiting the application of expanders is the significant temperature drop related to the conversion of internal energy of gas into mechanical work. It is therefore required to increase the amount of heat supplied to the gas prior to the expansion process. For industrial PRSs waste heat integration is a suitable option. For stand-alone PRS objects heat may be generated in gas boilers, or fuel cell systems (technology under development). Some authors also suggest to lead the process without pre-heating if the risk of hydrate formation is excluded. Moreover, low outlet temperatures may be used for cold generation if relevant process integration is possible [2].

After years of research, experimentation, COMOTI has developed a new configuration of turbine screw expander with oil injection (an advantageous solution for relatively small flows) that will have screw compressors advantages: high efficiency, due to the compression evolution nearly isothermal, low maintenance costs thanks to very good reliability, fewer moving parts, and not least competitive price. The solution has not been studied in Romania and is not applied to any plant or TRANSGAZ ROMGAZ stations. The advantages of using such equipment are, besides producing green electricity, natural gas availability to other consumers, reducing the amount of CO<sub>2</sub> released into the environment.

The pressure of natural gas in transmission pipelines before city gate stations (CGS) is high (5e<sup>7</sup> MPa). In order to utilize the potential energy of this high-pressure natural gas, power expanders are used to generate electricity or shaft work during natural gas pressure reduction. A small scale liquefied natural gas (LNG) plant may be also used in vicinity of pressure reduction plant to use the generated electricity to drive the compressors in liquefaction cycle. With gas pressure reduction, its temperature drops (JouleThomson effect), this may cause freezing of water vapor in natural gas which results in pipeline swelling and corrosion. The solution is to preheat the natural gas prior to pressure reduction. In order to gain even more electricity and savings, internal combustion (IC) gas engines may be utilized to drive additional generators and at the same time providing hot water in their water jackets for natural gas preheating. This equipment is categorized as a combined heat and power (CHP) system (a system which generates electricity and heat simultaneously using a single source of fuel). CHP systems play a significant role in efficient usage of energy in industrial and domestic applications. Furthermore, these systems have less harmful effects on the environment. Properly designed CHP systems may provide a thermal efficiency more than 80% [3].

## 2. PAPER CONTENTS

Expander was tested on the COMOTI's test bench, see Fig. 1. and at beneficiary Fig. 2. The testing program on the air, the experimental procedure followed, within the limits of available parameters from the stand. All measurements were recorded digitally and then transferred to a computer used for online processing, see fig. 3 the flow being discharged from the compressor is up to 1500kg / h and the expander inlet gas pressure reaching 15 bar.

The start is done by bringing the generator to synchronization speed by the helical expander followed by the connection to the grid and, compared with the synchronous machine, it is not necessary to consider the phase position (no special measures are required for its connection to the grid).



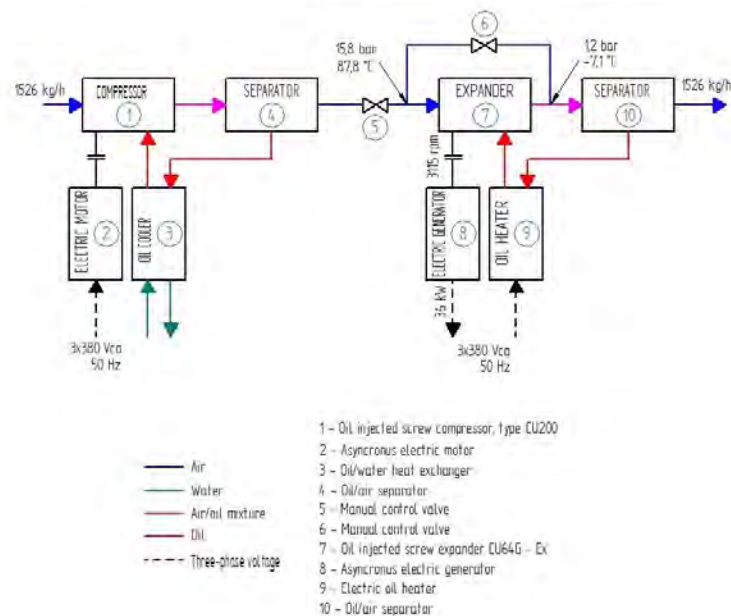
Fig. 1. Expander on the COMOTI's test bench



Fig. 2. Expander at the beneficiary

Making the asynchronous generator electrical connection with a 10% sync speed deviation results in a negligible influence on the electrical network connection.

After connecting the asynchronous generator to the grid, the new rotor speed value is set aperiodically, being determined by the ratio between the drive and generator moments. Thus, the fluctuations of active energy felt by the power grid become negligible [4].



**Fig 3. General diagram of connection of the 37kW expander-generator group in the stand of INCDT COMOTI with experimental parameters**

Acquisition of all parameters is done by a computer equipped with a data acquisition board. In the particular case of power consumed / debited a device, a network analyzer takes the values of currents and voltages on each phase, calculates and displays several electrical parameters, including the active power[5]. This is sent to the data acquisition board as a unified 4-20 mA signal, which through a proportionality ratio represents this power. The computer reads this signal, converts it into kW, displays it, and saves it on the HDD.

The operation of the expander-generator group is explained with reference to fig. 3 and the maximum power point obtained experimentally. The air is sucked at ambient temperature and pressure by the oil injection compressor 1. The compressor expels an air / oil mixture at high pressure and temperature in the air / oil separator vessel 4. The compressed and hot air is dosed through the tap 5 at a temperature of 87.8 ° C and a pressure of 15.8 bar at the aspiration of expander 7. Upon expulsion from the expander, the gas pressure is 1.2 bar. The pressure difference between suction and discharge causes the expander to rotate and provide an air flow of 1526 kg / h. The bypass valve 6 is partially closed in order to achieve a speed stabilization, the value obtained is 3,115 rpm. The resulting damping produces a mechanical power at the generator shaft which transforms the generator to 37 kW electric. That leads to lower gas pressures and temperatures. Adjusting the discharge temperatures is done with the hot oil used by the grease expander and the injection chamber. The heating of the oil is done with an electric heater. The expander expels an air / oil mixture from which oil is separated (in the gas / oil separator 10) to be reintroduced into the lubrication and injection circuit.

The graphical representation focused on 7 parameters with determination in achieving the energy performance of the asynchronous expander-generator group:

- Pga (bar), suction gas pressure;
- Pgre (bar), discharge gas pressure;
- Tga ( °C), suction gas temperature;
- Tgre ( °C), discharge gas temperature;
- P (kW), active power debited by the generator;
- N (rpm), generator speed;
- Qv (Nm<sup>3</sup>/h), the air flow entering the expander

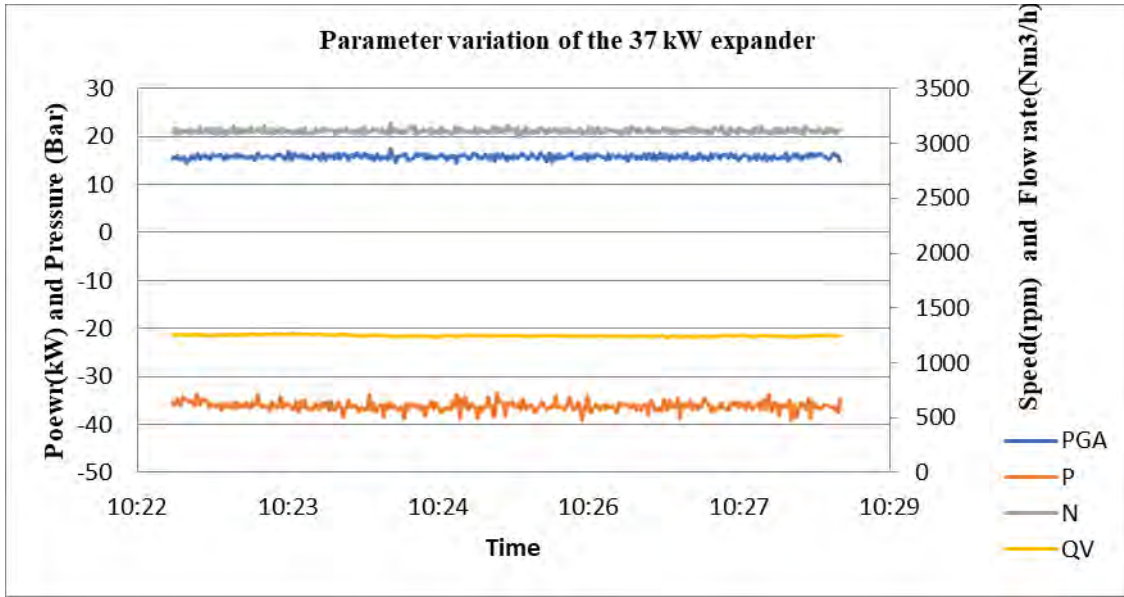


Fig. 4. The parameters of the 37 kW screw expander at COMOTI

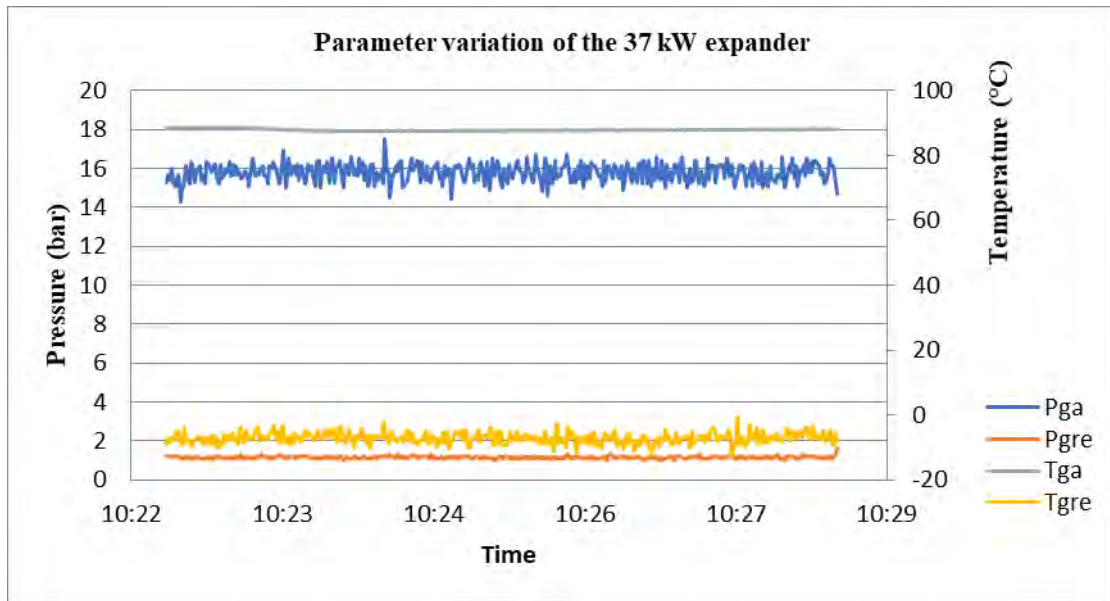


Fig. 5. The parameters of the 37 kW screw expander at COMOTI

The nominal system operating regime, Fig. 4., Fig. 5., for the electric generator - screw expander corresponds to the following parameters:

$p_1$  – pressure of the natural gas at the entrance of the expander = 15 bara;

$p_2$ – discharge pressure of the expander = 2 bara;

$\dot{m}$  - mass flow rate = 1500 kg/h = 0.416 kg/s;

$k$  –adiabatic exponent= 1,4;

$\eta_{iz}$  - isentropic expander efficiency = 0,7;

$C_p = k \cdot R/(k-1) = 1,010$  kJ/kgK

$R$  – gas constant = 287 j/kgK

$T_1 = T_{ga} = T_{ga}$  gas temperature suction = 80 °C = 353K

$$P_{ex} = G \eta_{iz} \frac{k}{k-1} R T_1 \left[ 1 - \left( \frac{p_2}{p_1} \right)^{\frac{k-1}{k}} \right] = 0,461 \times 0,7 \times 1,010 \times 353 \times \left[ 1 - \left( \frac{2}{15} \right)^{\frac{0,4}{1,4}} \right] = 41 \text{ kW} \quad (1)$$

$$P_{gen} = P_{ex} \cdot \eta_{gen} = 0.9 \times 41 = 36.9 \text{ kW} \quad (2)$$

$P_{ex}$  is the power generated at the expander shaft and  $P_{gen}$  is the power produced by the electric generator.

At the beneficiary the same testing procedure is followed, the working fluid is natural gas and the specific testing conditions were not suitable for the working parameters, and the testing procedures will be continued when the parameters will be suited for testing.

At the parameters of the station we obtained the following results, see Fig. 6 and Fig. 7.

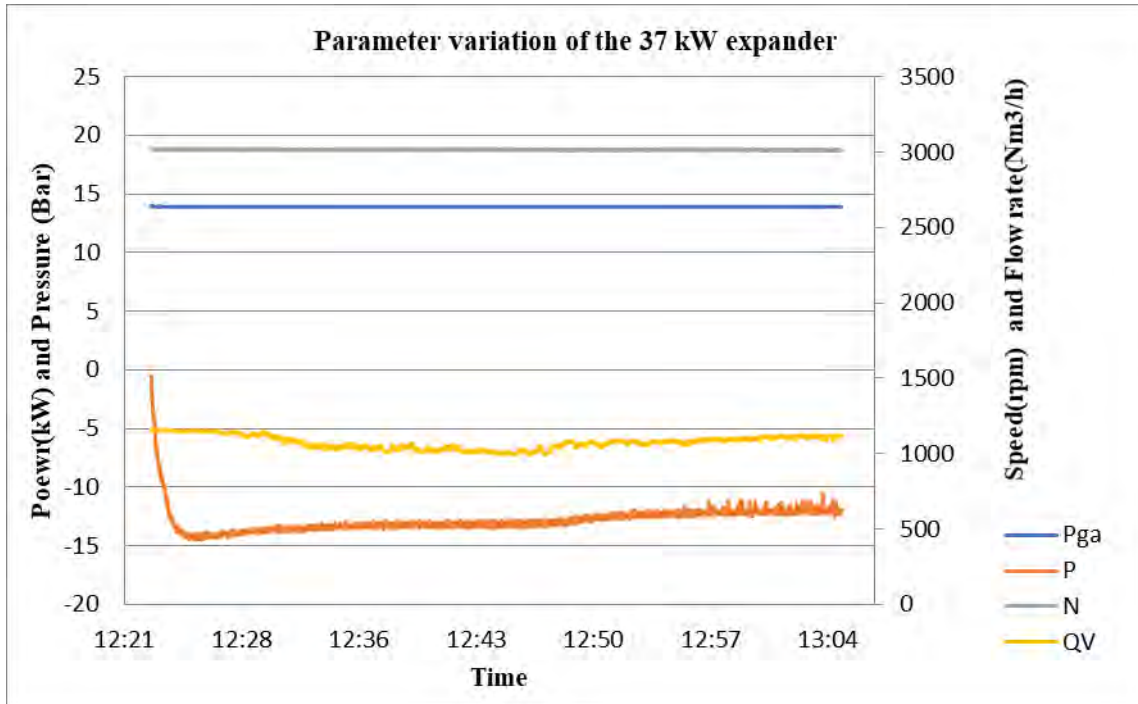


Fig. 6. The parameters of the 37 kW screw expander at beneficiary

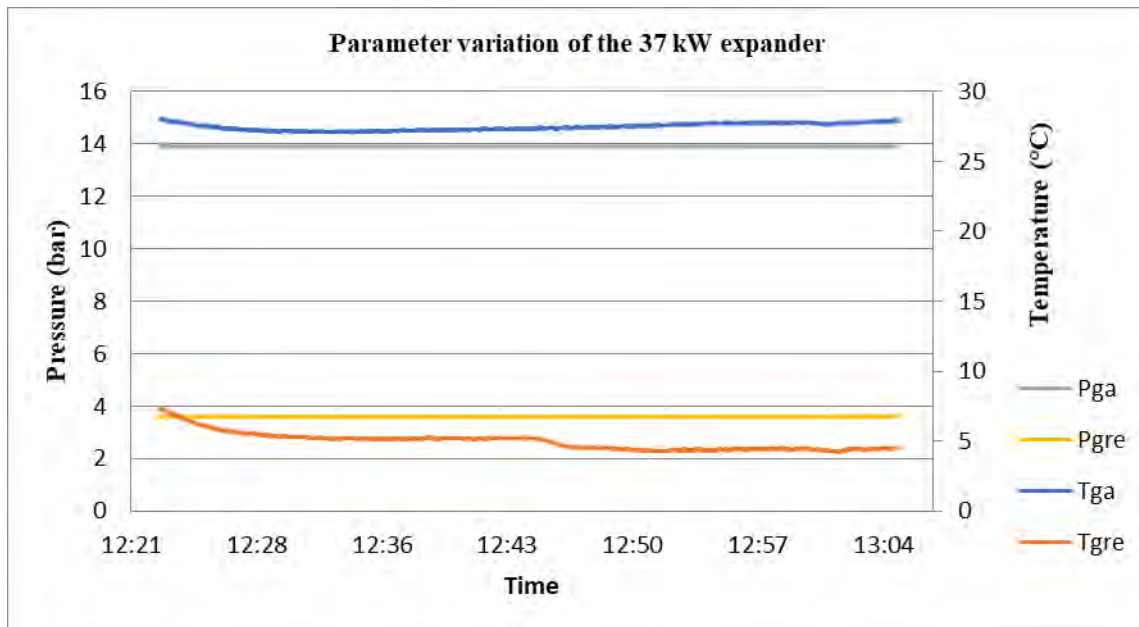


Fig. 7. The parameters of the 37 kW screw expander at beneficiary

### 3. CONCLUSIONS

I.N.C.D.T-COMOTI has developed an efficient equipment for the conversion of natural gas expansion energy into green electricity.

Benefits:

- High product efficiency due to almost isothermal expansion - by hot oil injection;
- High flexibility for variations of gas parameters at the suction of the expander;
- Minimum foundation due to continuous rotation and dynamic rotor balancing;
- Low maintenance costs due to very good reliability, low moving parts (constructive simplicity).

In Romania's energy development strategy, in order to increase the electricity supply security and to limit the import of energy resources, in the conditions of accelerated economic development, it is foreseen, among others, the implementation of a sustained energy conservation policy by maximizing its recovery from all available energy sources.

In the transport pipelines as well as in the control-measuring-delivery stations (SRM), the gas pressure must be reduced to the pressure required by the local system. Currently, this pressure adjustment is carried out by means of pressure regulators or rolling valves. The group contains the expander as a source to drive an asynchronous generator over synchronicity. The amount of energy produced is ensured by manually adjusting the gas flow rate injected into the expander.

### ACKNOWLEDGEMENTS

This work was carried out within "Nucleu" Program TURBO 2020, supported by the Romanian Minister of Research and Innovation, project number PN 16.26.02.03.

The results obtained during the scientific research activity were delivered at several scientific and professional conferences both in Romania and abroad, and they materialized into an invention patent: Equipment for power production **no. 125674**, diplomas and medals received at international exhibitions:

- Equipment for power production: **IENA, Nuremberg 2012 - Gold medal**;
- Equipment for power production: **Eureka 2012 – Silver medal**;
- Equipement pour la production d'énergie: **Geneve 2013 – Gold medal**.
- Energy efficiency, essential condition for a sustainable development **Meda conference 2017**,

**Bucharest**

- Capitalizing on renewable energy in the transport of natural gas in National Transportation System, by optimizing the performance of the elicoidal expander -electric generator control group **CEAS 2017**

### REFERENCES

- [1] TOMA N., 2007; "Turbina cu surub, Forumul de gaze naturale", Editia a II-a, Sibiu, Romania
- [2] WOJCIECH J. Kostowski a,† , SERGIO Usón b, 2012, "Thermoeconomic assessment of a natural gas expansion system integrated with a co-generation unit" Applied Energy Volume 101, January 2013, Pages 58-66
- [3] SEPEHR Sanaye, AMIR Mohammadi Nasab, 2012, "Modeling and optimizing a CHP system for natural gas pressure reduction plant"; Energy Volume 40, Issue 1, April 2012, Pages 358-369
- [4] TOMA N., 2009, "Sistem producere energie electrica", Forumul de gaze naturale Editia a III-a, Bazna, Romania
- [5] TOMA N., 2010; "Recovery of the gas energies expansion by electrical power production for low gas flow, TechnoForum of OMV Petrom E&P2nd" Edition: Compressors Days, Ploiesti, Romania
- [6] TOMA N., 2010; "Solutie moderna de recuperare a energiei de detenta a gazelor prin utilizarea expanderelor", Drilling and production servicing seminar, Bucharest, Romania

# FAULT DIAGNOSIS OF AIRCRAFT GAS TURBINE ENGINE BY VIBRATION ANALYSIS

Lică FLORE<sup>7</sup>

**ABSTRACT:** The experimental identification of mechanical system of aircraft engine is achieved through a detailed research of the engine vibration behavior. The instrumentation and signal processing technologies existing today determine more precisely the required parameters for the calculation of engine lifetime than theoretical calculations. These parameters have a big impact on the operational safety and the maintenance process of aircraft. The experimental vibration analysis area is extensive and involves several other fields: vibration measurement, signal processing, mathematics and statistics, problems on systems vibration with several degrees of freedom, different damping models, etc. This work focuses on finding and applying reliable methods for the experimental identification of mechanical structures of aircraft gas turbine engine. The first step on the identification process is the definition of the type of experiments to be done (or experimental model). The purpose of the experimental model must to be clearly defined at the beginning because it affects the experimental conditions. The experimental identification of the dynamic behavior consists on finding of the transfer function, also called frequency response function (FRF), which best describes the mechanical components of the engine analyzed.

**KEYWORDS:** Vibrations, Gas turbine, Frequency spectrum, Fault diagnosis, Regression,

## NOMENCLATURE

C	Damping matrix
FFT	Fast Fourier Transform
FRF	Frequency Response Function
$H(\omega)$	Transfer function
Im	Imaginary part
K	Stiffness matrix
Re	Real part
TV2	Klimov gas turbine engine
Vb	Vibration level
c, $\alpha$	Damping factor
$f_i$	Frequency [Hz]
$f(t)$	Excitation force
j	Complex unit
m	Mass
t	Time
$x, \dot{x}, \ddot{x}$	Displacement, Velocity, Acceleration
$\Omega_0$	Resonance frequency [rad/s]
$\omega$	Angular frequency [rad/s]

## 1. INTRODUCTION

The aim of predictive maintenance is first to predict when equipment failure might occur, and

<sup>7</sup> National Research and Development Institute for Gas Turbines COMOTI, Bucharest, Romania

secondly, to prevent occurrence of the failure by performing maintenance. Monitoring for future failure allows maintenance to be planned before the failure occurs. Ideally, predictive maintenance allows the maintenance frequency to be as low as possible to prevent unplanned reactive maintenance, without incurring costs associated with doing too much preventative maintenance.

The typical vibration analysis using modern equipment and techniques starts with the acquisition of the variable signals in the time domain from a standard vibration sensor (accelerometer is most commonly used) with high accuracy. The raw analog signal is brought to equipment that processes it in a variety of ways. If the analysis of waveform is done through digitization, it is necessary to choose the number of samples and the sampling frequency. Almost all vibrations analysis equipment include the FFT (Fast Fourier Transform) device as a general way of transforming the analog signal into the individual frequency components. There are several parameters to setup the FFT process: resolution, maximum frequency, averaging, averaging number, type of window, etc. All these parameters affect the desired result, being a compromise between the quality of information and the time needed for data acquisition.

The experimental study of vibration phenomena presents several approaches, but in practical terms, the following situations can be mentioned [1]: *signal analysis* which provides the type and level of the system vibration response, *system analysis* which involves the development of the theoretical models and the vibration behavior estimation of the system. As a consequence, there are two types of the experimental measurements according to the approaches above: *diagnosis* when the vibration response of the structure or machine under investigation is measured during operation, *modal tests* when the structure as a whole or only parts of it, are put into a vibration state and its response is measured.

A significant shortening of the testing time is necessary. To achieve this, a new procedure, called testing strategy, was introduced recently in the management for vibration diagnosis. The target of this procedure is, on the one hand, to reduce the volume of data and, on the other hand, to use an analytical preliminary view to eliminate non-relevant modes of vibration.

The main interests of the study carried out during the development of this work were the assessment of the efficiency and accuracy of various experimental methods, the exploration of the possibility of using different types of transducers and measurements in the processes of signal acquisition and processing. The exploration and comparison of several methods of signal processing, the assessment and analysis of the differences between vibration parameters, estimated through numerical methods and those obtained through experimental methods, are explored. The processing of the test parameters is a fundamental part in the field of gas turbine engine fault diagnosis. The evolution of computer programs enables for complex analysis and advanced data processing.

## 2. ENGINE VIBRATION MEASUREMENT

### 2.1. Existing Techniques for Vibration Monitoring of Aircraft Gas Turbine Engines

Standard methods of engine vibration monitoring involve comparison of recorded engine vibration levels with fixed operational limits set by engine manufacturers, or vibration signature, which derive from an engine of the same class as that used, in order to detect sudden shifts in operational behaviour, often indicators of potential failure.

Some of the data processing techniques of fault diagnosis by vibration measurements used in the field of aircraft engine, with different degree of applicability, are presented below:

*Peak-picking method*, suitable for structures whose frequency response functions show the vibration modes well isolated and have moderate damping. The identification procedure through this method are briefly summarized as follows: recording of the FRF curve and observation of its peaks, calculation of the damping at the peak frequencies, estimation of the modal shapes from the ratio between the maximum amplitude of the different points of the structure and the maximum amplitude of the reference sensor.

*Circle fitting method*, benefits from the behavior of most systems in the vicinity of the resonance frequency. This behavior is dominated by a single mode of vibration [2]. Through this method, the accuracy of the obtained values at resonance is acceptable, except the damping factor, which cannot be measured with a good accuracy as through the previous method. The method uses the complex plane to represent the real and imaginary components of a signal.

It should be noted that any forced elastic deformation of a engine structure can be represented as a weighted sum of its modal shapes; each eigen mode can be represented as a system with one degree of freedom (SDOF). This is the basic element of the vibration analysis. Any engine part can be analysed through the identification and assessment of the resonances that occur in the response spectrum. In any measurement method, the following aspects demand special attention in order to ensure a high quality data acquisition: mechanical



aspects of supporting, correct conversion of the quantities to be measured and signal processing, appropriate to the type of the test used.

### 2.2. Theoretical Background

Independently of its complexity, any structure is assimilated to a number of masses connected to each other by springs and damping elements. The inertial and elastic forces can be measured with sufficient precision but the damping forces can only be estimated. Any estimation of the damping forces can be done assuming that if the excitation force is harmonic, the damping forces are also harmonic.

The systems with one degree of freedom (SDOF) are very rare in practice, but the theoretical bases of the modelling for these systems are valid for systems with multiple degrees of freedom (MDOF) through the linear superposition hypothesis. The MDOF system can be assimilated with a sum of multiple systems with one degree of freedom. In this case, the equation that describes the system motion is a matrix equation with an order equal to the number of degrees of freedom [33]. The equation of the damped system motion with one degree of freedom with a disturbing force is:

$$m \cdot \ddot{x}(t) + c \cdot \dot{x}(t) + k \cdot x(t) = f(t) \quad (1)$$

and has the solution:

$$x(t) = \left\{ \frac{1 - \left(\frac{\omega}{\Omega_0}\right)^2}{\left[1 - \left(\frac{\omega}{\Omega_0}\right)^2\right]^2 + \left(2\alpha \frac{\omega}{\Omega_0}\right)^2} - j \cdot \frac{2\alpha \frac{\omega}{\Omega_0}}{\left[1 - \left(\frac{\omega}{\Omega_0}\right)^2\right]^2 + \left(2\alpha \frac{\omega}{\Omega_0}\right)^2} \right\} \cdot \frac{F_0}{k} e^{j\omega t} \quad (2)$$

or :

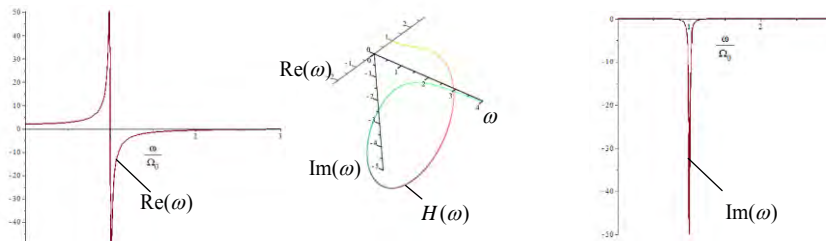
$$x(t) = \text{Re}(x(t)) + j \text{Im}(x(t)) \quad (3)$$

where:  $\text{Re}(x(t))$  and  $\text{Im}(x(t))$  represent the real and imaginary components of the system response, according to the pulsation  $\omega$ .

These functions provide the response signal and the response signal phase, for any frequency, proportional with the level of excitation signal:

$$FRF = \frac{FFT(response)}{FFT(excitation)} \quad (4)$$

Any of these functions contains all the necessary information to identify the vibration behavior. The problem is having enough response magnitude for processing [5]. Therefore, the measurements of the response and excitations in several points of the structure are required.



**Fig. 1 Theoretical graphical representation, using the Maple program, of the movement components with frequency  $\omega$ :**

The 3D representation of frequency response function (FRF), corresponding to a system with one degree of freedom, is illustrated in the next figure. The orthogonal projections of the FRF represent the real signal part, the imaginary signal part and gain factor, also called Nyquist diagram.

The simulation of the mechanical structure real behaviour, in terms of damping, through the finite element method (FEM) involves the introduction in the program of some arbitrary parameters. The current progress in the synthesis and acquisition field of the signals makes from the experimental method for assessing the damping factor an important aid in the determination of the input parameters in numerical method. Such complementarily between experimental and numerical methods was applied in this work.

Starting with Rayleigh hypothesis, [3] where the damping matrix is given by:

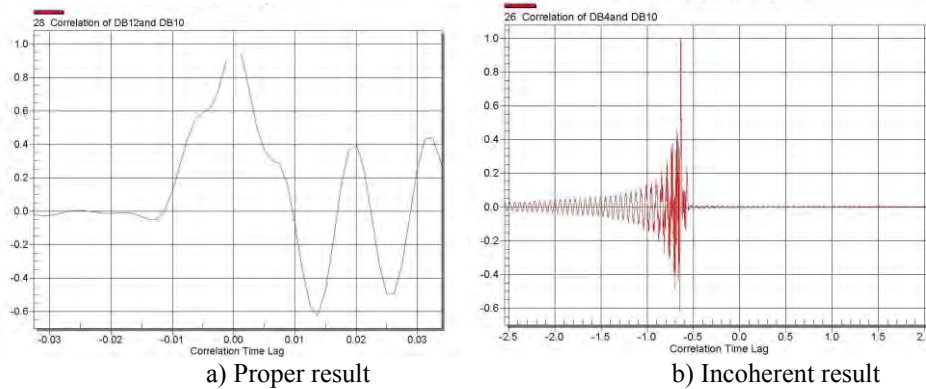
$$[C] = \sigma[M] + \beta[K] \quad (5)$$

Where  $\sigma, \beta$  are factors which can only be determined through the experimental method, we can find:

$$\sigma = \frac{2f_i f_{i+1}}{f_{i+1}^2 - f_i^2} (f_{i+1} \alpha_i - f_i \alpha_{i+1}) ; \quad \beta = \frac{2}{f_{i+1}^2 - f_i^2} (f_{i+1} \alpha_{i+1} - f_i \alpha_i) \quad (6)$$

where  $f_i, f_{i+1}$  are two consecutive eigen frequencies which can be determined through experimental methods.

The signal processing in the experimental vibration measurements is performed using the signal analysers with multiple channels. There are several ways [4] to calculate the response for linear and nonlinear systems. At least two channels are necessary because the simultaneous processing involves two signals: excitation (speed) and response (vibration level). The response spectrum is often contaminated by other factors such as noise. It is obvious that the mathematical apparatus, however perfect it could be, is not able to distinguish true vibration modes from false vibration modes. To distinguish them, the operator's experience or the preliminary knowledge about the real modes of the structure, obtained from a theoretical model, are necessary. The work performed have to includes a wide approach on the digital processing errors caused by the effects of noise and the phase change effect between excitation forces and acceleration response. The coherence function, which indicates the degree of linearity between input and output signals (Fig. 2), have to be used in order to minimize the errors. The specific features of aliasing, leakage and weighting windows have to be also discussed.



**Fig. 2 Examples of coherent and incoherent results during vibration measurements**

### 3. FAULT DIAGNOSIS ANALYSIS

The proposed fault diagnosis system was developed and tested with actual TV2 engine data collected from the Comoti's test cell in startup phase. The startup of a gas turbine engine from ignition to idle speed is very critical for health monitoring of many subsystems involved. During startup, an engine goes through a number of phases during which various components become dominant [5]. The proposed approach physically monitors the relevant phases of a startup by detecting distinct changes in engine behavior as it manifests in such critical variables as the core speed and the vibration level. Keeping the size of the data needed for the fault diagnosis much smaller than that of the complete data is another reason (more advantageous and much more efficient). The continuous idle profile can be represented by several points, without losing its characteristics, Fig. 3. The second step in data processing is to choose the typical engine start profile (signature) and then to estimate the predictive vibration level by polynomial regression method (Fig. 4).

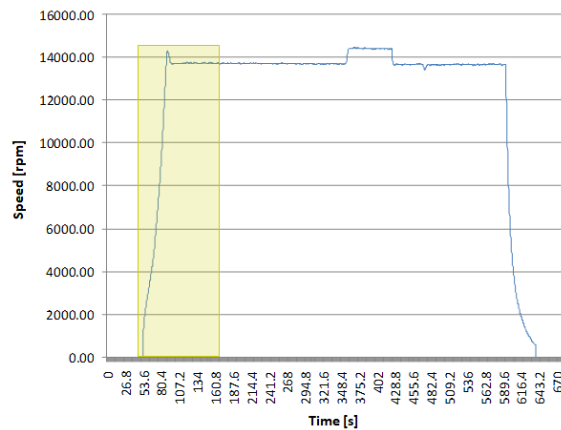


Fig. 3 The data selected range for processing of fault diagnosis analysis

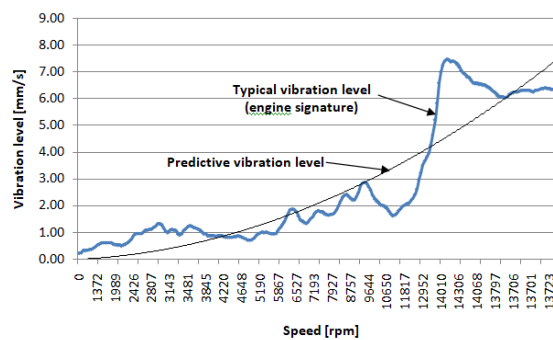


Fig. 4 Typical evolution and evolution trend of the vibration level in startup phase of TV2 engine

The state of the art in monitoring engine is that engine parameters are sampled at regular frequencies and compared against fixed thresholds on these parameters. Often, the thresholds are set arbitrarily by monitoring these parameters, at different engine speed, in test cell. Sometimes, the thresholds are set by experts or based on design specifications. In either case, startup monitoring does not capture the changes in engine response accurately and in a timely manner. For this reason, is necessary to fix the acceptable limits (+/-15% in this case). Figure 5 presents the features that show the distinguishable signatures between the abnormal and normal TV2 startup engine behavior obtained by vibration measurement.

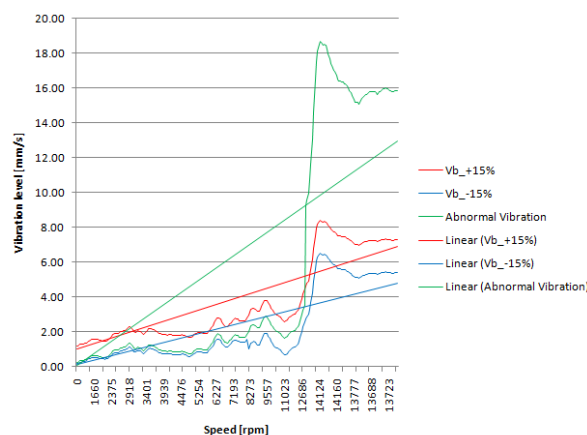


Fig. 5 Example of the fault diagnosis (simulation) by comparison vibration level with the acceptable limits.

The last step in data processing is to processing in order to obtain logical value in according with engine maintenance manual or other procedures. The partial result of vibration level analysis on TV2 gas turbine engine, in order to detect an abnormal behaviour, is shown in Table 1.

**Table 1. Assignment of fault logical value after comparing the current vibration level with typical level**

Time (s)	Vb (mm/s)	Vb +15% (mm/s)	Vb -15% (mm/s)	Vb simulation (mm/s)	Logical value
33	2.17	3.12	1.22	2.17	normal behavior
33.2	2.27	3.22	1.32	2.27	normal behavior
33.4	2.42	3.37	1.47	2.42	normal behavior
33.6	2.63	3.58	1.68	2.63	normal behavior
33.8	2.98	3.93	2.03	2.98	normal behavior
34	3.23	4.18	2.28	3.23	normal behavior
34.2	3.52	4.47	2.57	3.52	normal behavior
34.4	3.69	4.64	2.74	9.22	bearing failure
34.6	3.83	4.78	2.88	9.57	bearing failure
34.8	3.98	4.93	3.03	9.96	bearing failure
35	4.28	5.23	3.33	10.70	bearing failure

Usually the transducers are mounted on various points of the engine assembly for the measurement of engine vibration level. Vibration data, used for investigations described in this paper, were acquired using a system that computes Fast Fourier Transforms (FFT) representative of engine vibration every 0.2 seconds. The engine vibration is assumed pseudo-stationary over this measurement period such that the generated FFT are assumed to be close of actual engine vibration power spectrum.

#### 4. CONCLUSIONS

The vibration behaviour of a mechanical structure is sufficiently characterized without knowing the internal construction of such structure (distribution of mass and stiffness) if the vibration tests fulfil certain requirements. According to the work results, carried out during the study, a successful predictive maintenance by vibration monitoring requires a combination of theoretical framework, accurate measurement of vibration and realistic and detailed data processing. This paper provides the method to condense the data required to characterize engine dynamics from several hundred seconds to about two dozen data points per test phase, which has tremendous implications in engine health monitoring. This approach to on-board acquisition allows real-time data transfer and makes timely prognostics possible.

This paper is focused on research of frequency domain spectral data. However, time domain data also contains information that may be exploited for the diagnosis of engine abnormality. A model of normal signal behaviour may be constructed using auto-regressive deviations from which could identify abnormal conditions. Time-frequency analysis of engine data combines both domains for a more complete representation of engine state, describing the evolution of the spectral content of a signal through time.

Using of the preliminary experimental determinations necessary in numerical simulation method by calculation of the damping factor, through Rayleigh hypothesis, from two consecutive eigen frequency values, can be useful. The complementarities between experimental measurements and numerical simulations, in order to achieve the closest model to the real mechanical engine structure in terms of vibration behaviour, are already common practice in predictive maintenance of aviation structures. The signal acquisition process depends on several key elements of the adaptation and the conversion of data: the overall level of vibrations, the amplitude levels, the signal frequency acquired and the signal phase relative to the excitation signal.

In order to maximize information from engine vibration measurements the shaft speeds can be quantised. A number of data compression schemes need to be investigated to ensure that sufficient information is retained to allow abnormal engine behaviour to be identified using statistical estimation. Therefore, the further researches can be focused on data compression, improved abnormality detection and data fusion.

#### ACKNOWLEDGEMENT

This work was carried out within “Nucleu” Program TURBO 2020, supported by the Romanian Minister of Research and Innovation, project number PN 16.26.03.03. Some of the experimental results, which are presented in this paper, were obtained in the Testing Laboratory at Straero SA.

## REFERENCES

- [1]. Lica Flore, 2016, Contributions to experimental aircraft systems identification based on measured data and advanced processing of response signals, PhD thesis, University Politehnica of Bucharest, Faculty of Aerospace Engineering;
- [2]. Bilošová Alena, 2011, Modal Testing, Ostrava, Czech Republic;
- [3] Fuiorea, I., Flore L., Gabor D., 2012, A point of view upon rayleigh damping hypothesis, "Aerospatial", ISSN 2067-8622, Bucharest, pag.1-13;
- [4] Peter Avitabile, Modal Analysis and Controls Laboratory, 2010, University of Massachusetts Lowell;
- [5] Kyusung K., Onder U., Girija P., 2005, Fault Diagnosis of Gas Turbine Engine LRUs Using the Startup Characteristics, Proceedings of ASME IDETC 2005. September 24-28, Long Beach, CA ;
- [6] Stefan Walter, November 2011, Introduction to Modal Analysis, Hamburg University of Applied Sciences, Fakultät Technik und Informatik.



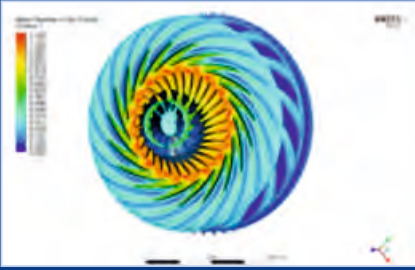
**COMOTI**  
ROMANIAN RESEARCH &  
DEVELOPMENT INSTITUTE FOR  
**GAS TURBINES**

220D Iuliu Maniu Ave., 061206 Bucharest, ROMANIA,  
P.O. 76, P.O.B. 174

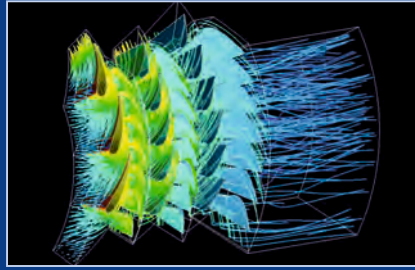
Phone: (+4)021/434.01.98, (+4)021/434.02.31, (+4)021/434.02.40  
Fax: (+4)021/434.02.41, e-mail: [contact@comoti.ro](mailto:contact@comoti.ro)

[www.comoti.ro](http://www.comoti.ro)

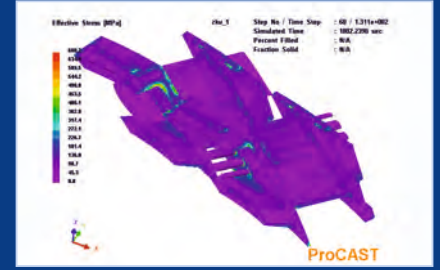
# COMOTI Capabilities & Expertise



Centrifugal rotor CFD applications.



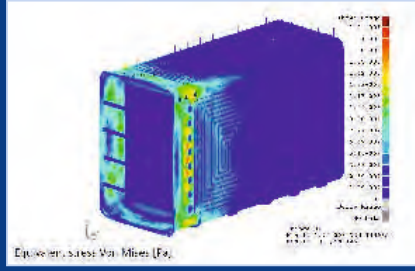
Gas turbine CFD applications.



Casting FET applications.



Planetary gear box 3D design.



FEA low pressure thermal box.



Gas turbine engine 3D design.



HAAS grinding CNC.



Centrifugal rotor on MCNC.



Centrifugal rotor.



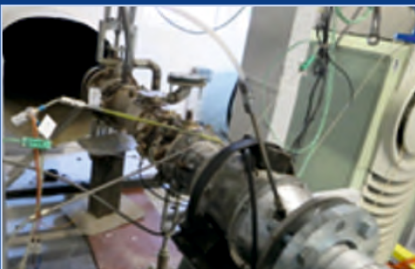
Wide range thermal test facility.



DELTA 34.04 CMM.



Anechoic chamber.



Combustion test rig.



Gas turbine engine test rig.



Micro turbjet for target plane.



Screw compressor skids station.



Centrifugal blower skid.



Centrifugal compressor skid.



The only specialized company that integrates  
such activities as

scientific research,  
design,  
manufacturing,  
testing,  
experimental activities,  
technologic transfer and  
innovation

in the field of aircraft and industrial gas turbines and  
high speed bladed machinery.

220D Iuliu Maniu Ave., 061206 Bucharest, ROMANIA,  
P.O. 76, P.O.B. 174

Phone: (+4)021/434.01.98, (+4)021/434.02.31, (+4)021/434.02.40  
Fax: (+4)021/434.02.41, e-mail: [contact@comoti.ro](mailto:contact@comoti.ro)

[www.comoti.ro](http://www.comoti.ro)